

Blazar Variability Research and Observations by Weihai one Meter Telescope

Shao Ming Hu (胡紹明)

Institute of Space sciences, Shandong University at
Weihai

Dec. 4, 2017, Kagoshima, Japan



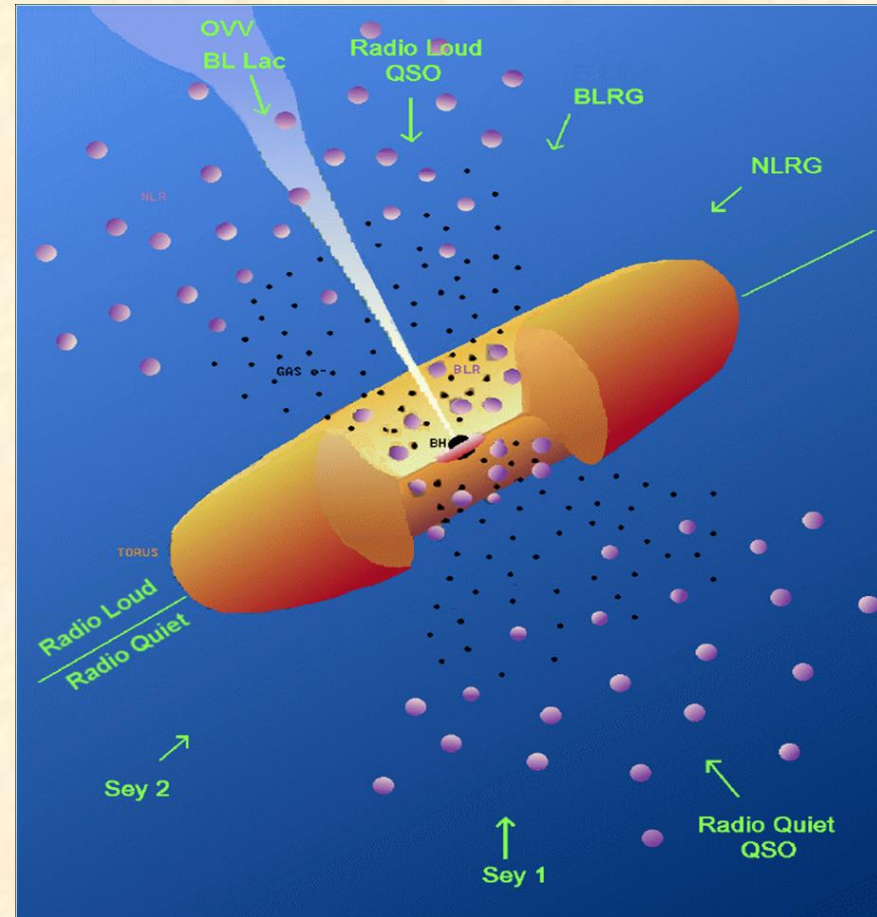
Outline



- Motivation
- Brief introduction to Weihai observatory
- Blazar observations and variability research

Blazars

- Defined by 1) strong variability (minutes to years) from radio to γ -rays and high polarizations (1-4%)
- Moderate to strong radio sources (radio loud)
- Two classes:
 - 1) **BL-Lac objects**: no strong emission or absorption lines
 - likely beamed FR Is
 - 2) **Optically-violent** variables (OVVs): highly polarized, variable, but have broad emission lines like quasars
 - likely beamed FR IIIs

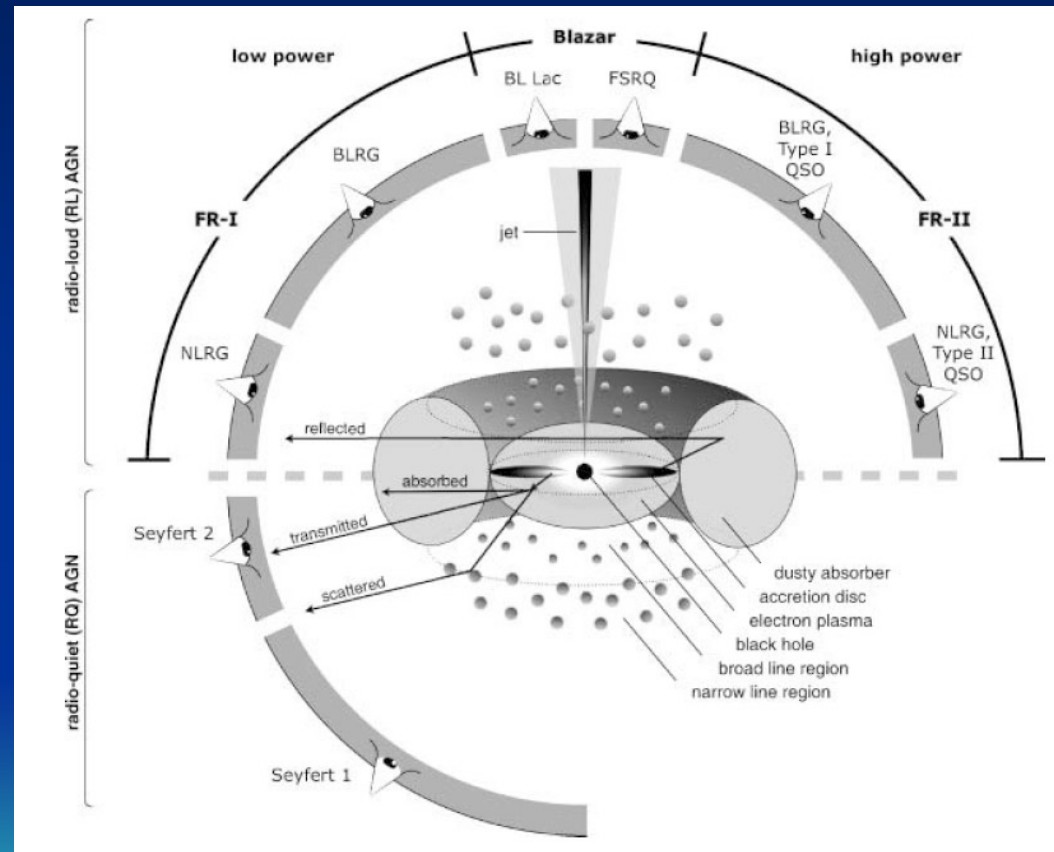




Research Motivation



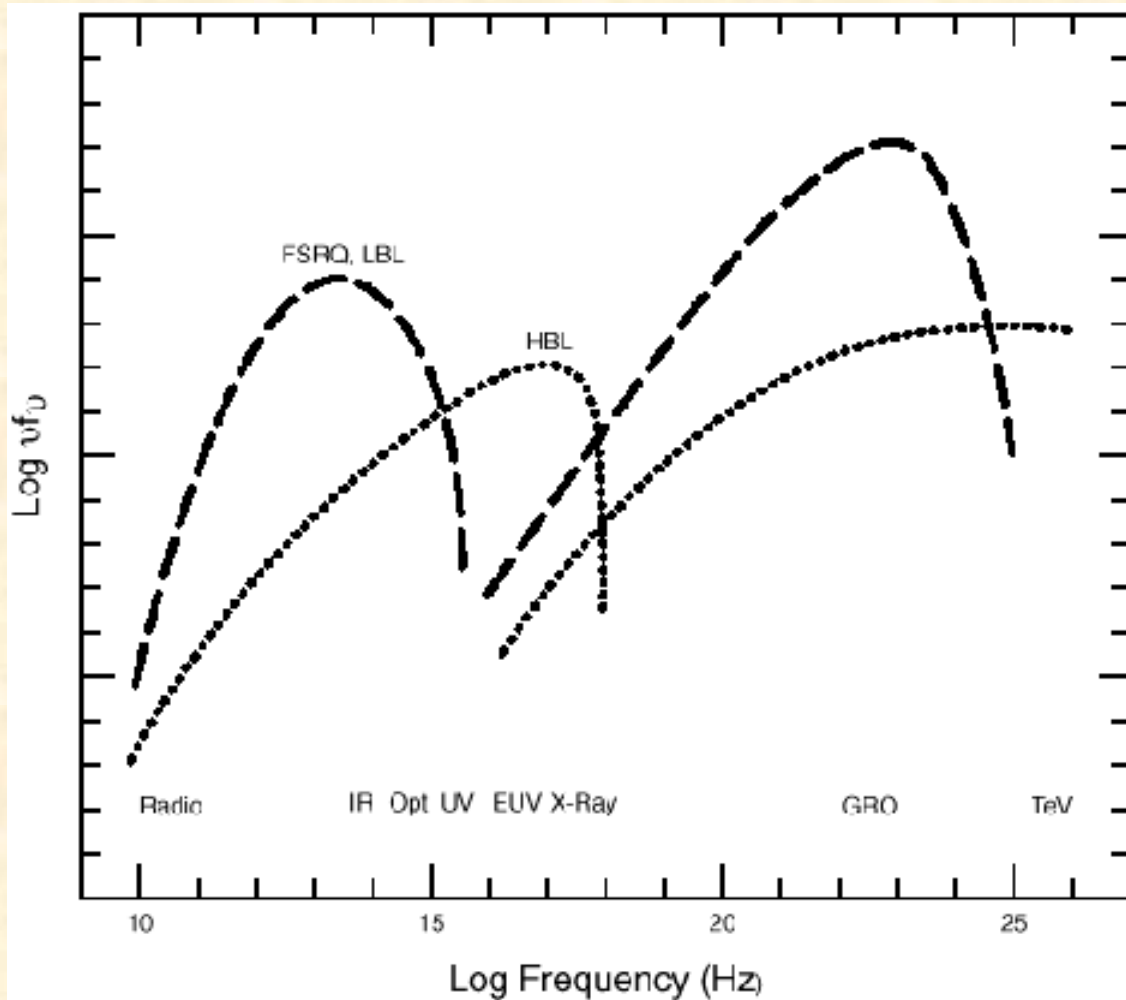
- The structure of BH, Accretion disk, BRL etc within pc can not be observed directly. Variability is an important method to research the central structure and physical process of AGN;
- Blazar is a natural lab to research the physics of jet;
- The origin of blazar variability is still an open question. More observational properties are needed to understand the origin and physics of AGN variability.



(Netzer 2015, ARA&A, 53, 365; Wagner & Witzel 1995, ARA&A, 33, 163; Ulrich et al. 1997, ARA&A, 35, 445; Falomo et al. 2014, A&ARv, 20, 73)

Blazar SEDs (Urry 1998)

Synchrotron Inverse Compton



Inverse Compton Models:

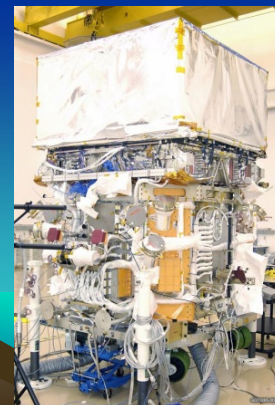
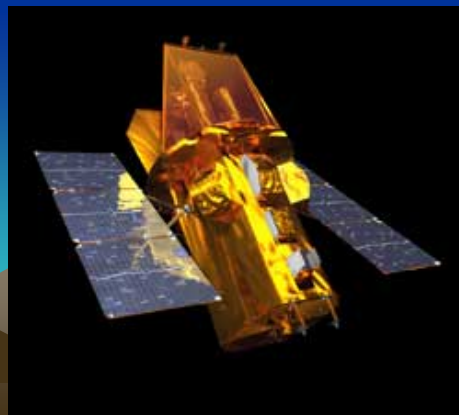
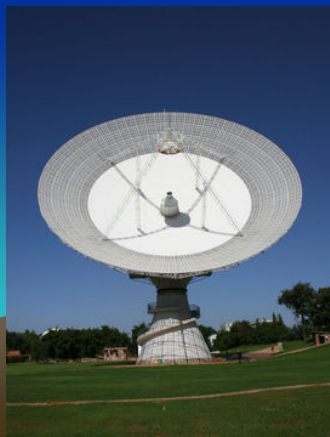
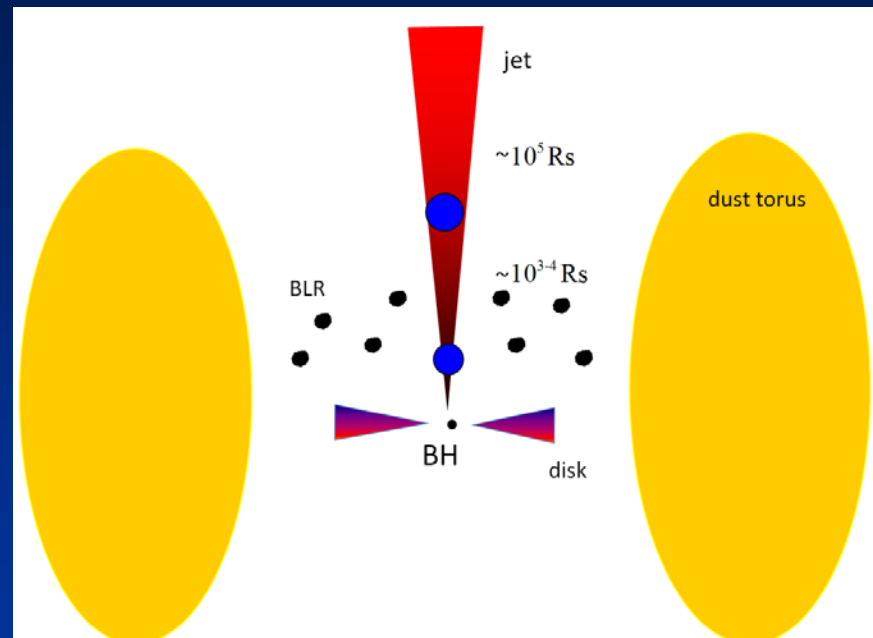
- Synchrotron Self Compton (SSC)
- External Compton (EC): seed photons from accretion disk, BLR, Cosmic Microwave Background (CMB), etc.



Research Motivation



- ◆ Blazar has radiation across the complete electromagnetic spectrum. Multiband variability properties and information are probes to understand the central structure, energy origin and mechanism, jet physics etc.;
- ◆ It's possible to research by multiband information due to open Radio, IR, optical, SWIFT, Fermi etc. data.





Observational research on variability properties



Observation
analysis

Variability
properties

Variability
origin and
physics

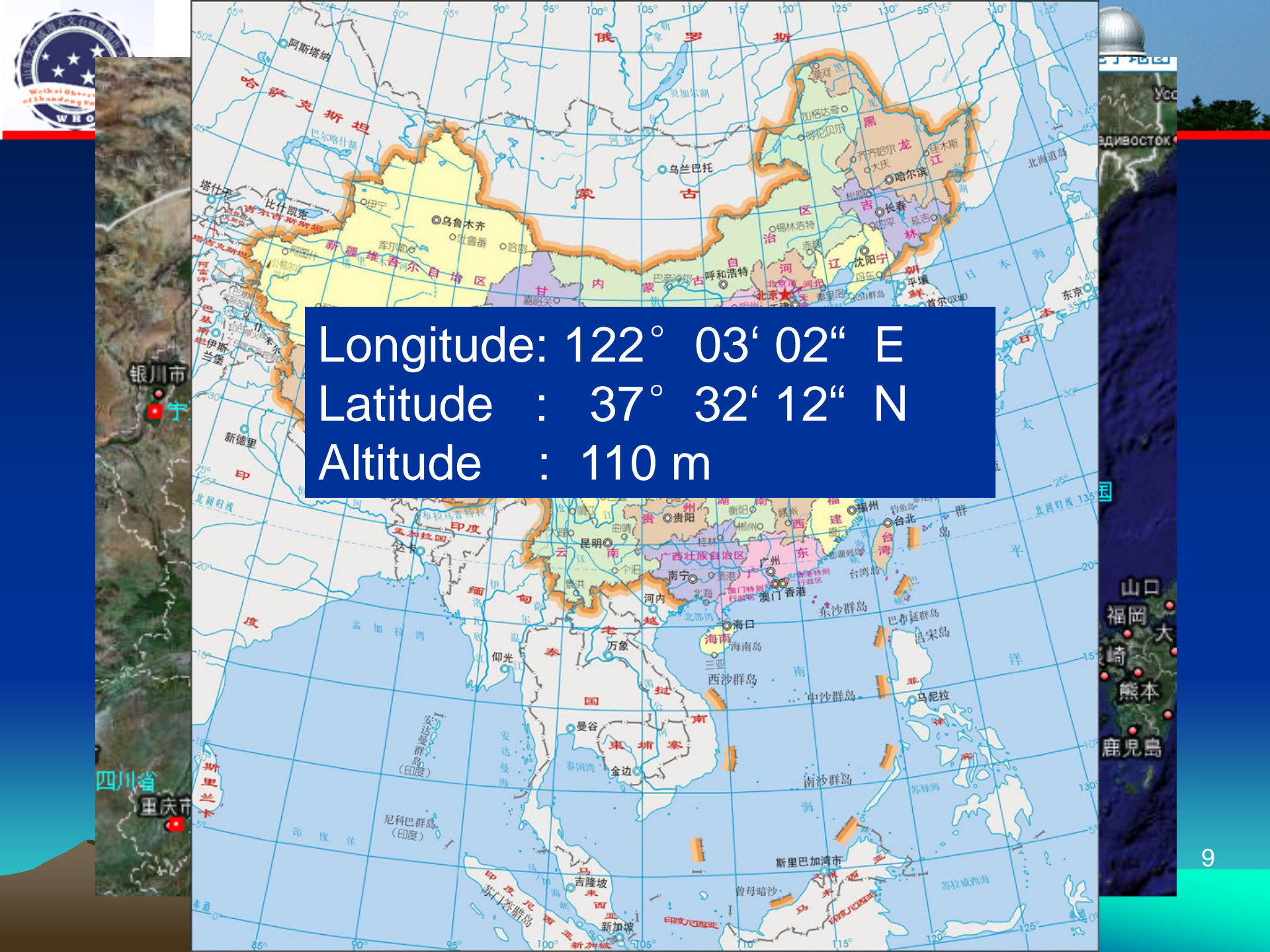
- Spectra variability
 - Microvariability properties
 - Variability symmetry
 - Periodic variability, the time scale, energy of flares.....
-
- Constrain the radiation mechanism
 - Provide physical parameters for physical models
 - Constrain the physical process and accretion mechanism in jet.....



Outline



- Motivation
- Brief introduction to Weihai observatory
- Blazar observations and variability research

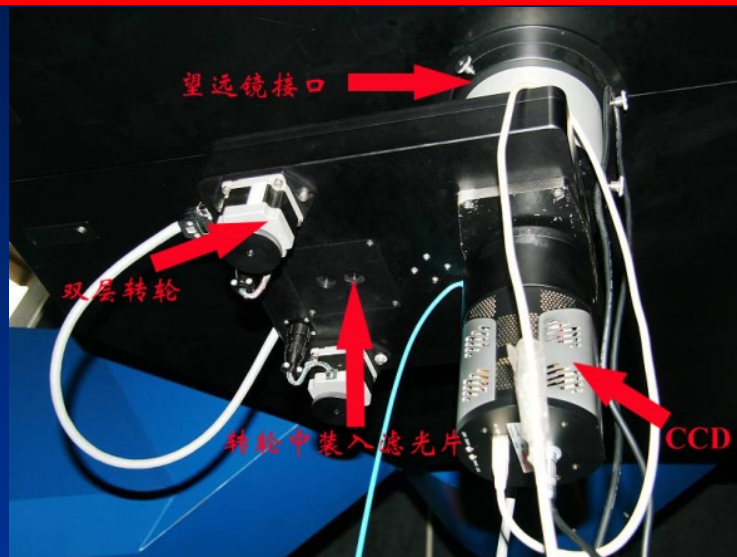


Longitude: 122° 03' 02" E
Latitude : 37° 32' 12" N
Altitude : 110 m

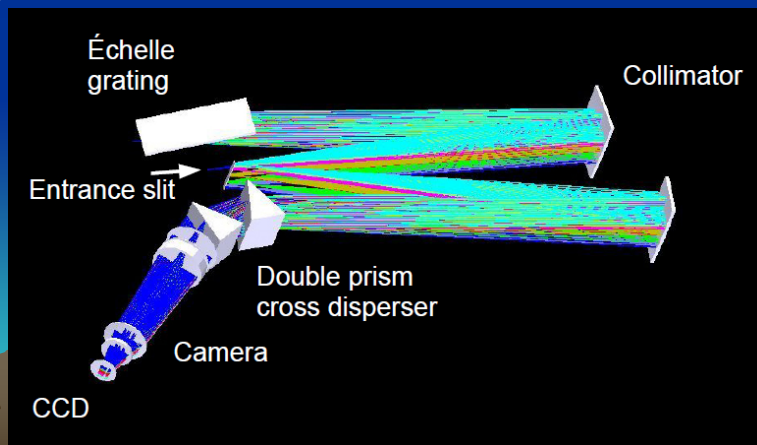


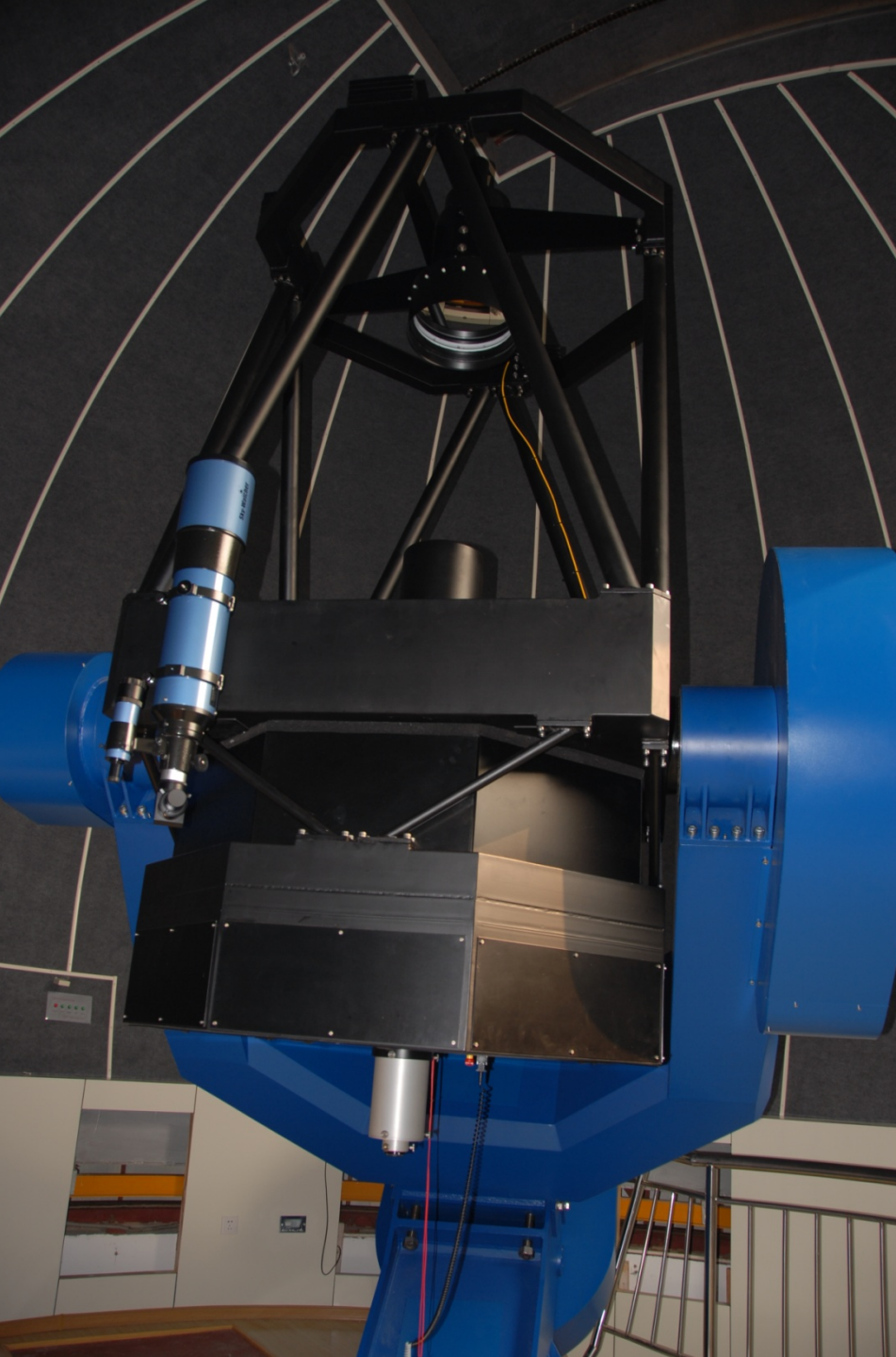


Instruments



Two
Instruments





Telescope

Optics: classic Cassegrain design, 1000mm optical working diameter, focal ratio: f/8

Mount: equatorial fork mount

Image quality: 80% Energy in 0.65 arc sec within 15 arc minute FOV

Maximum slew speed is 4 degrees per second in both RA and DEC axis

Pointing accuracy: 5.4 arc sec RMS for 20-90 deg altitude

Tracking accuracy: 0.54 arc sec RMS in 10 minutes blind guiding

Photometry system

望远镜接口



双层转轮



转轮中装入滤光片



CCD



CCD Camera

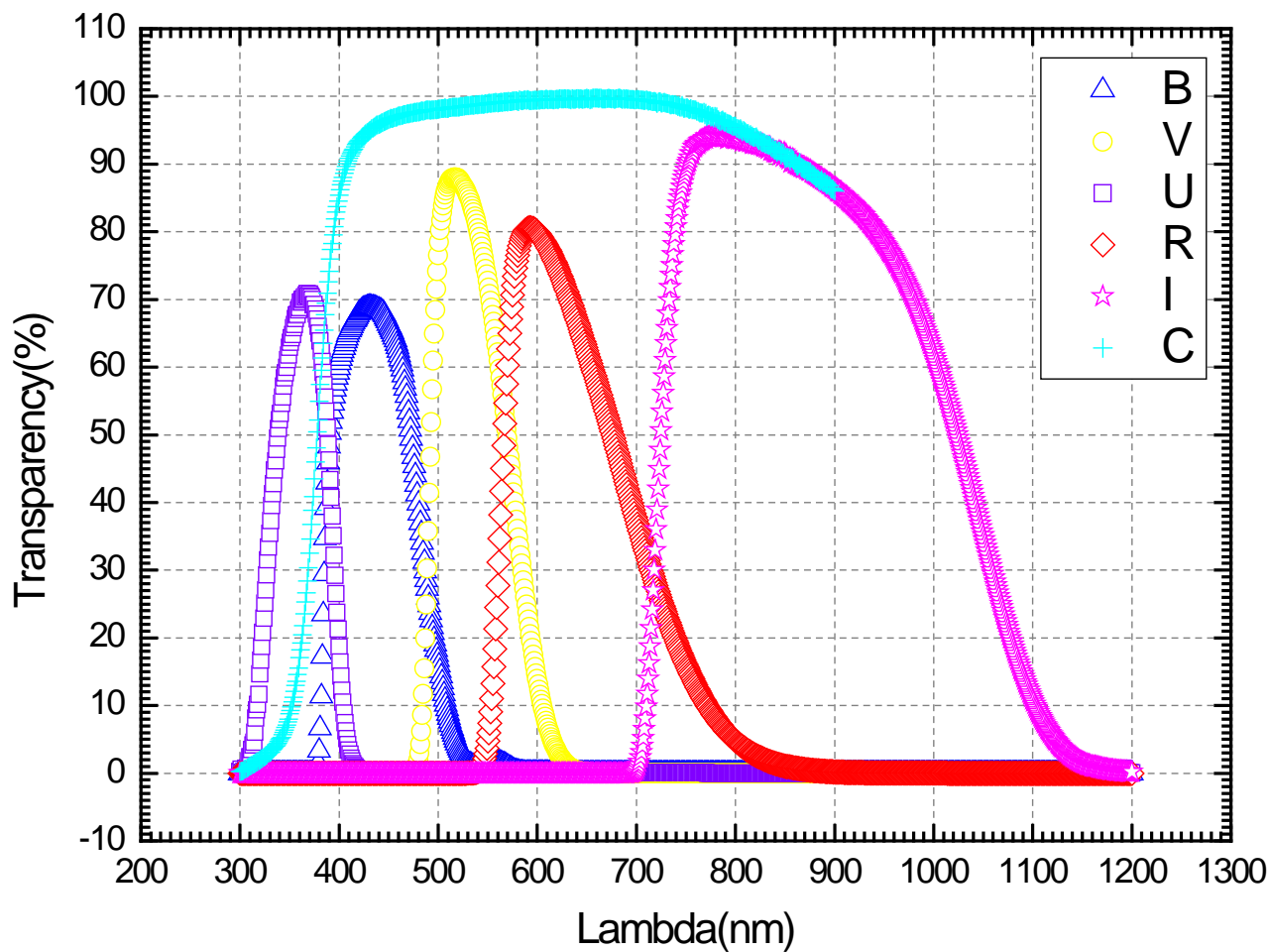


PIXIS 2048B



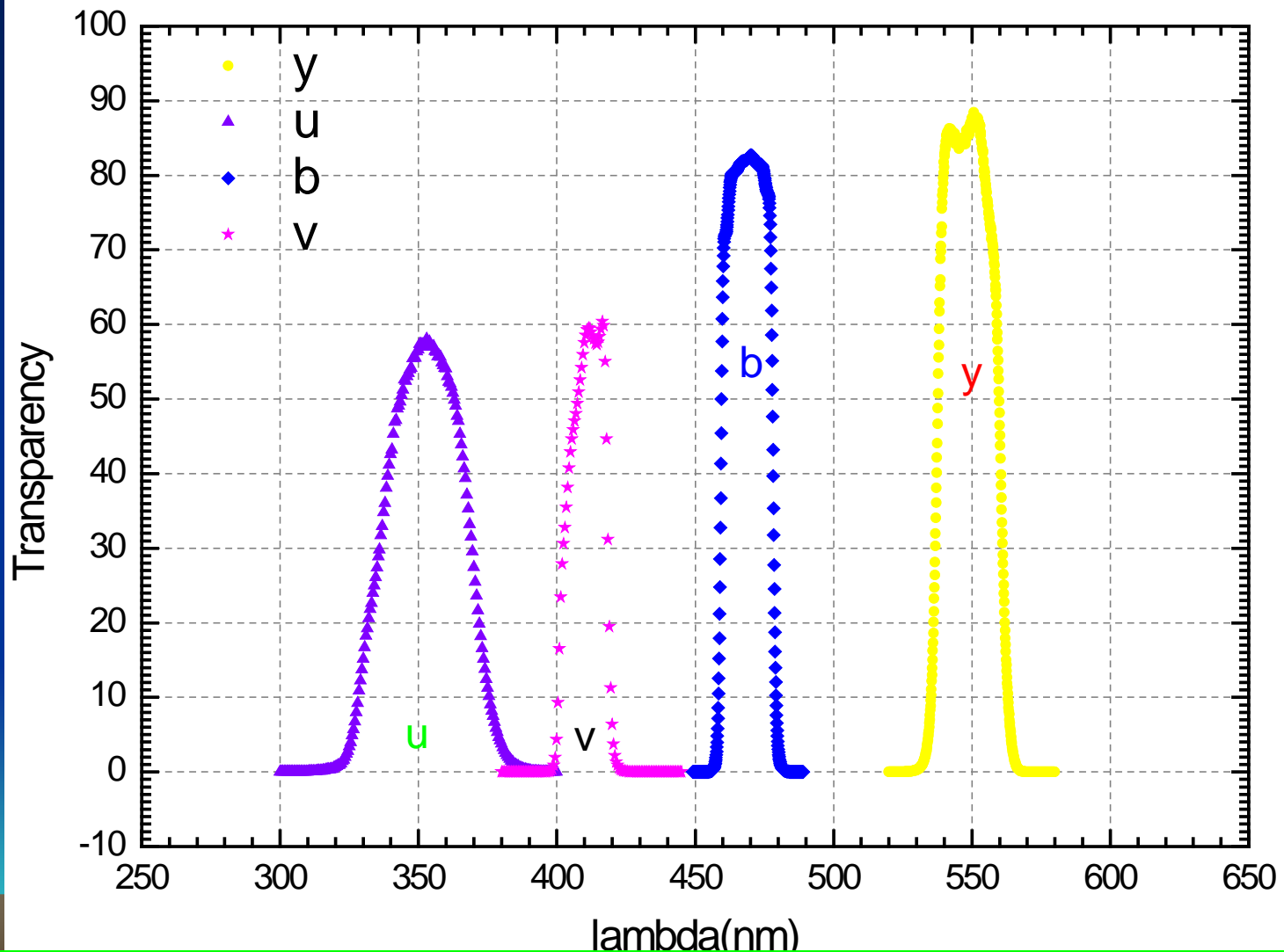
Andor iKon-L DZ936-BV

Filters



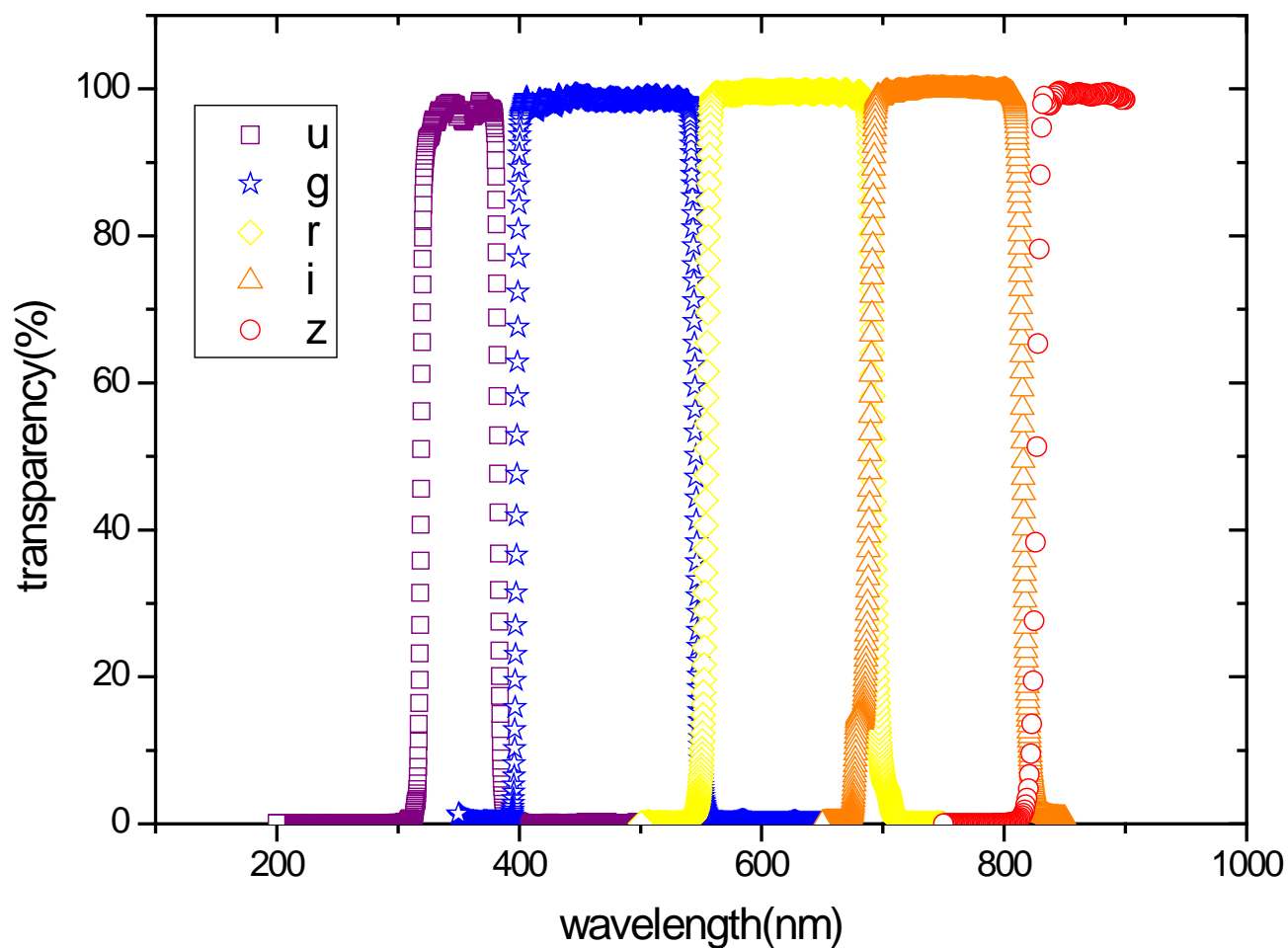
Transparency of Bessel UBVRIC filters

Filters



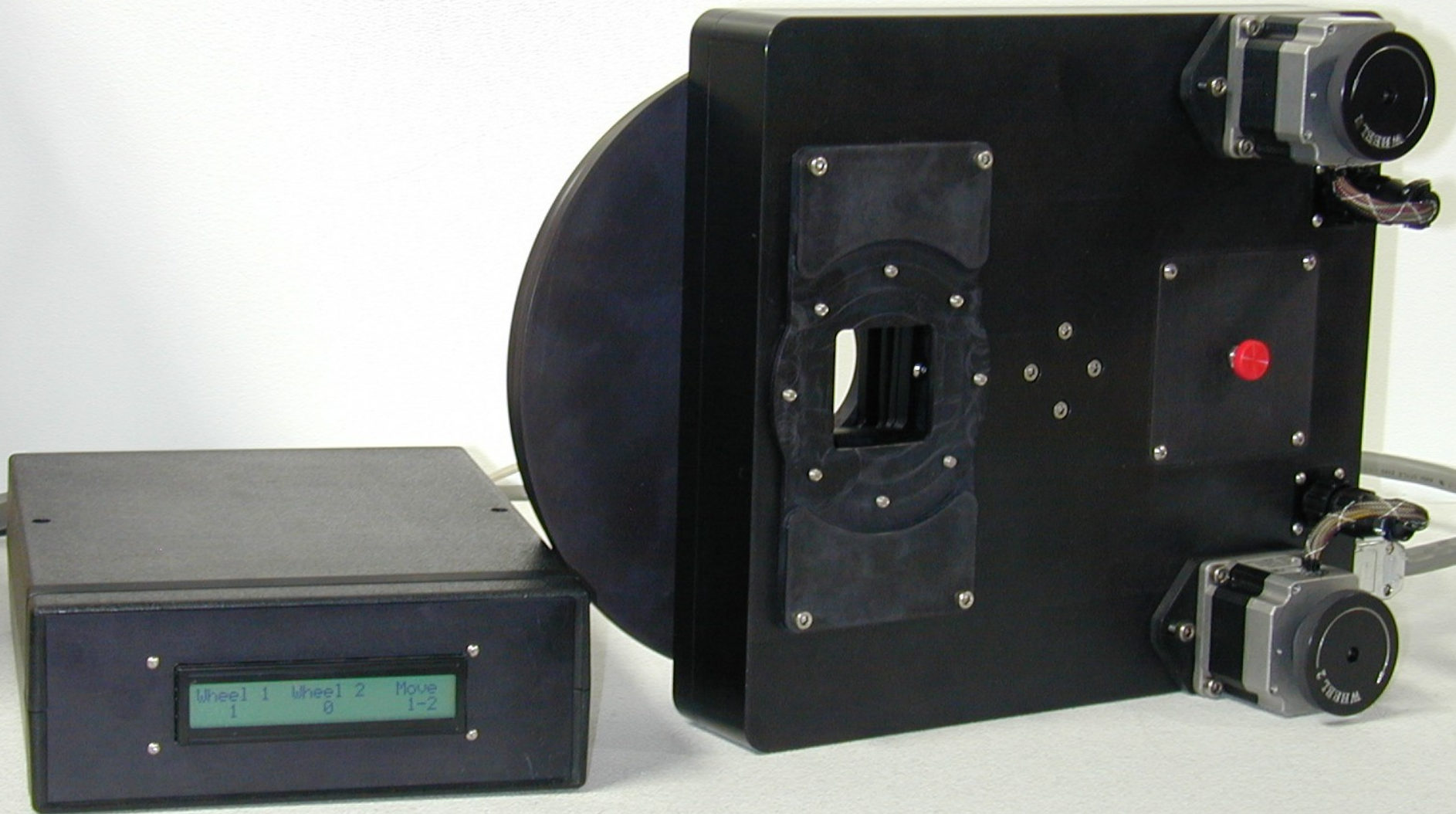
Transparency of Stromgren filters

Filters





Filter wheel



ACE Dual filter wheel

Seeing

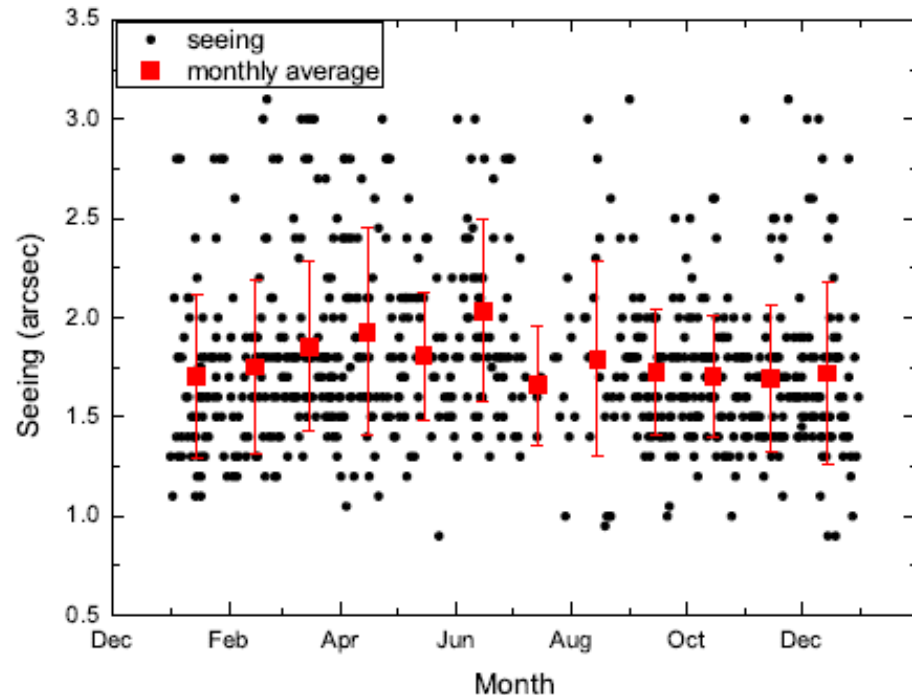
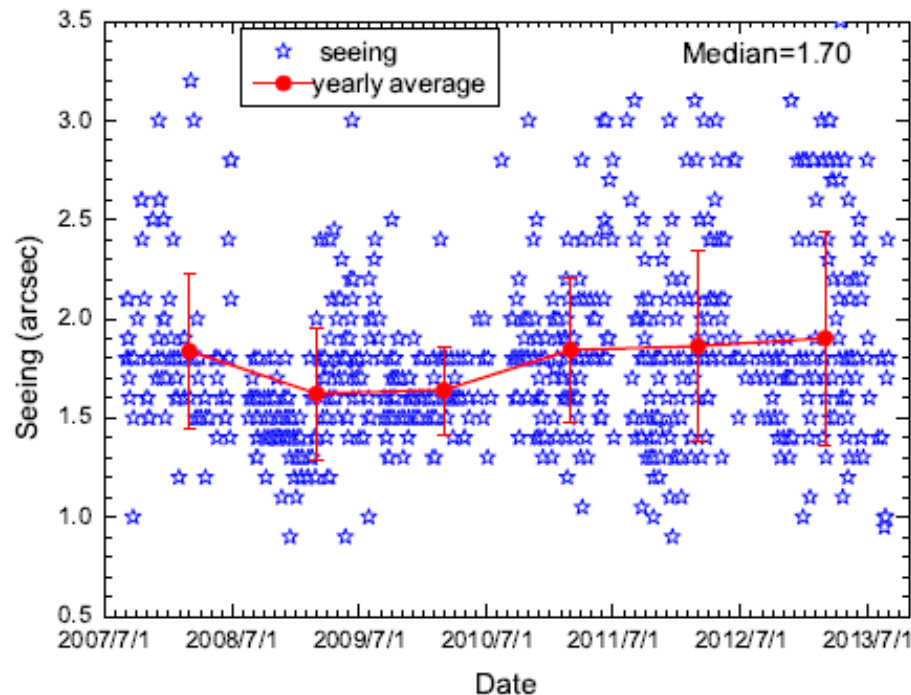
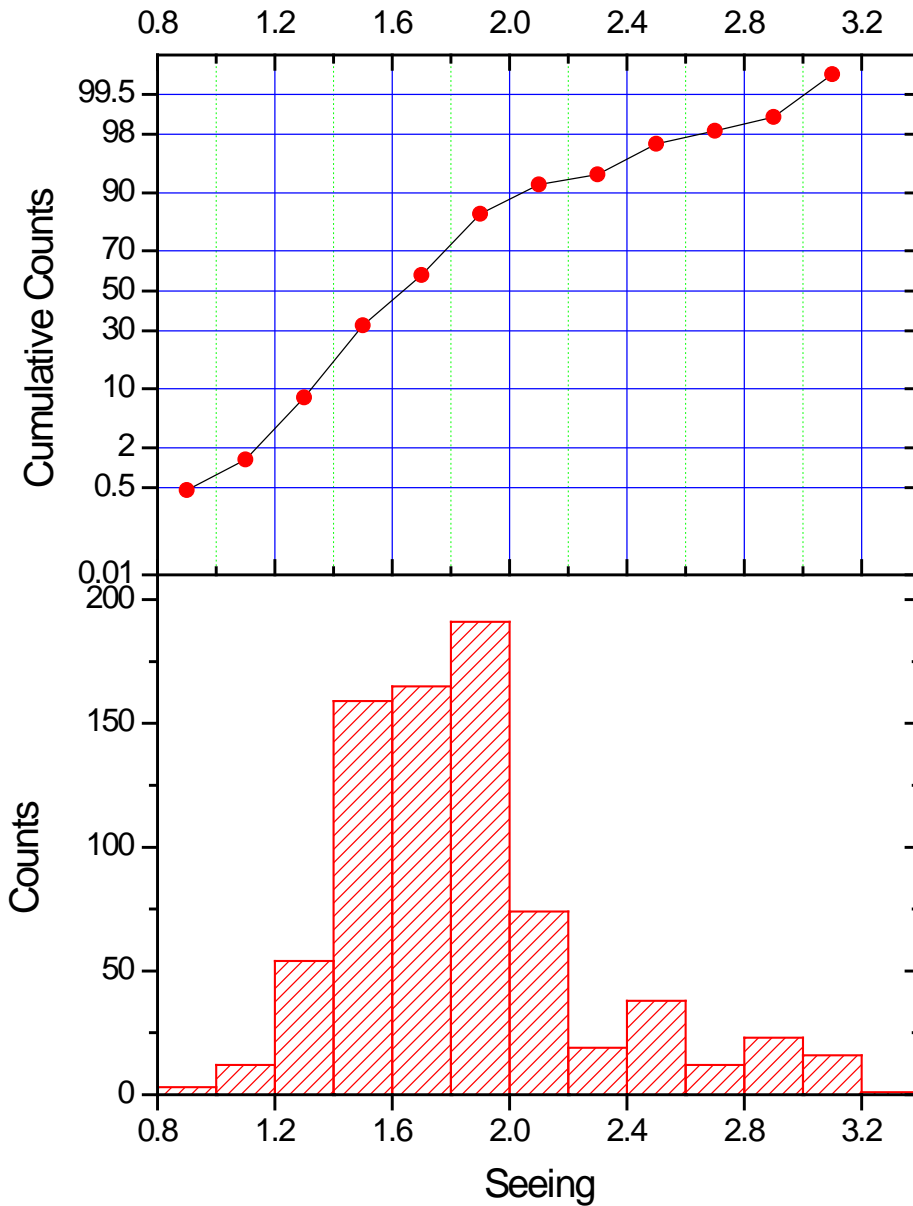


Fig. 2 *Left:* Seeing versus observation date in the past six years. Red dots describe the yearly average of the seeing. *Right:* Seasonal variation of seeing. Red solid squares illustrate the monthly average values for seeing.

FWHM measured by images.(768 nights, almost 6 years) see Hu et al., RAA, 16, 719, 2014.

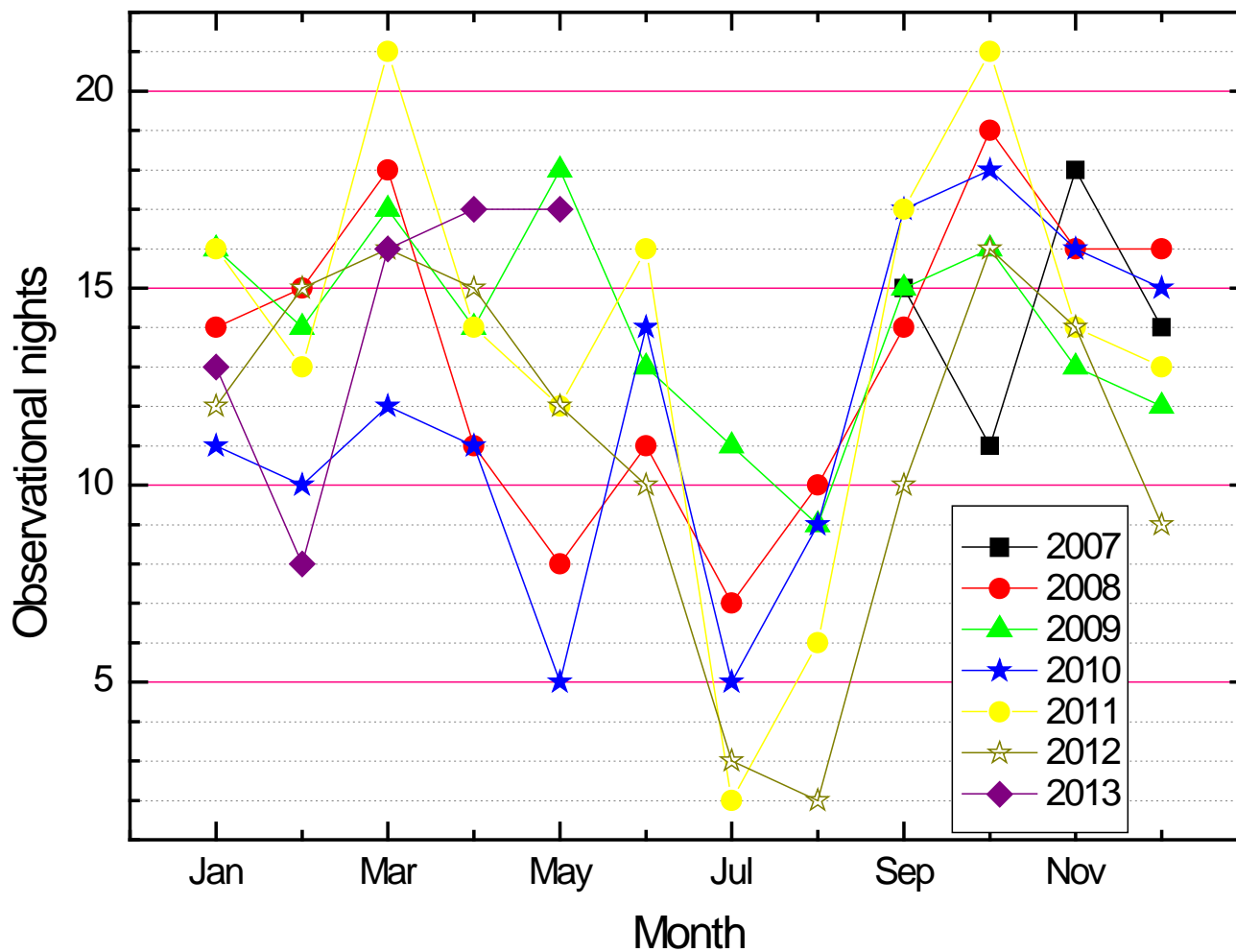
Seeing



Statistic result of seeing, 90% seeing is better than 2.0 arcsecond



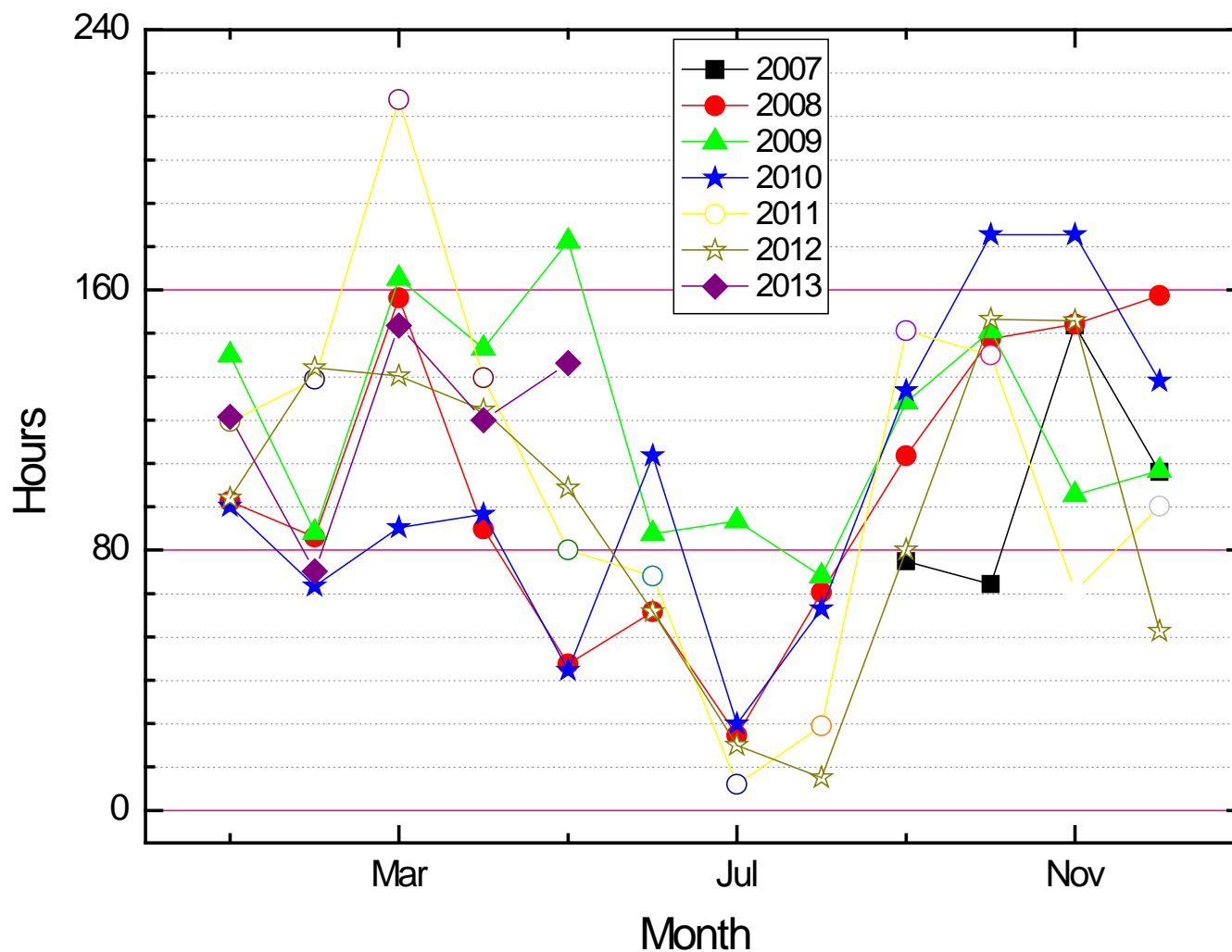
Weather condition



Monthly observatinal nights

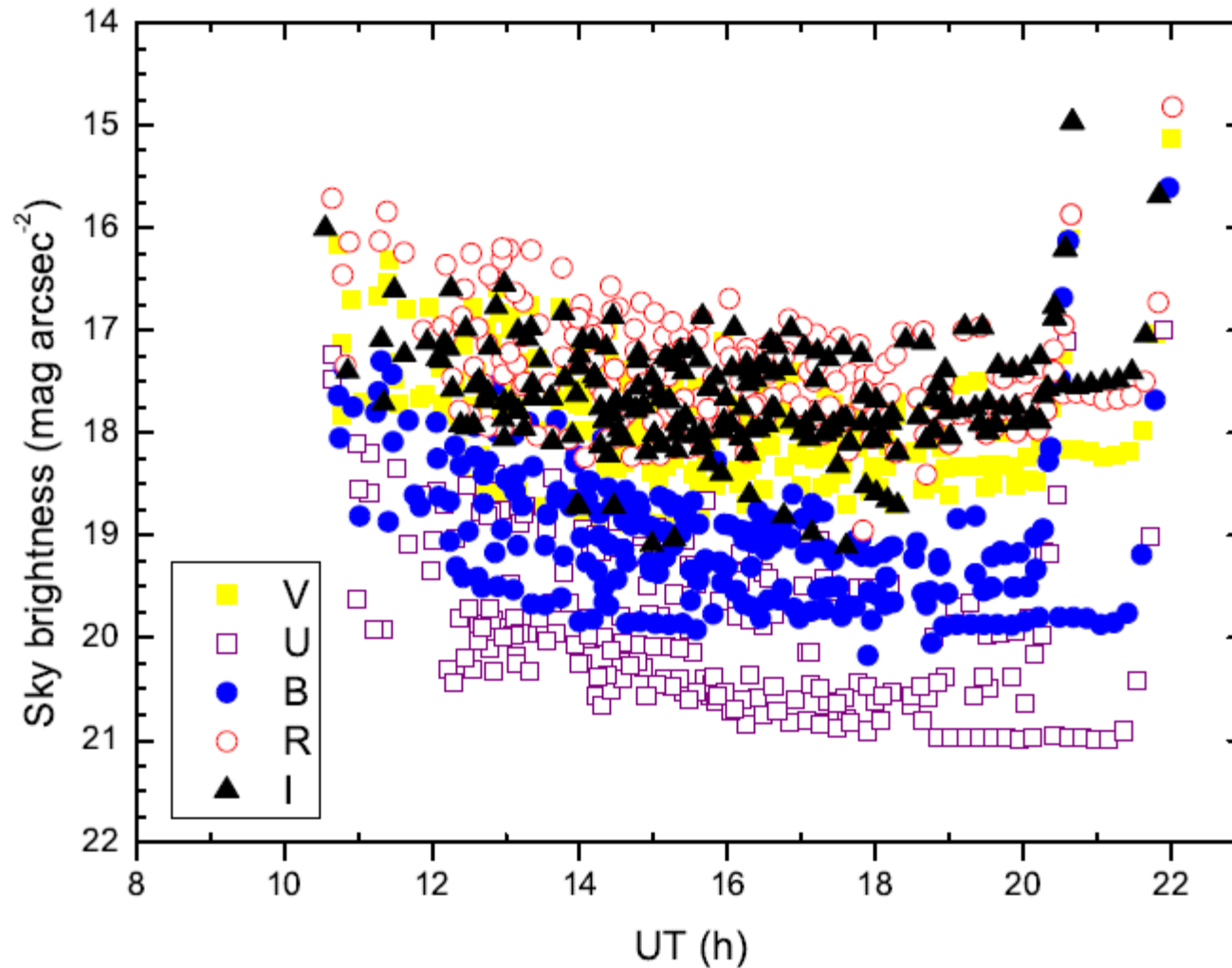


Weather condition



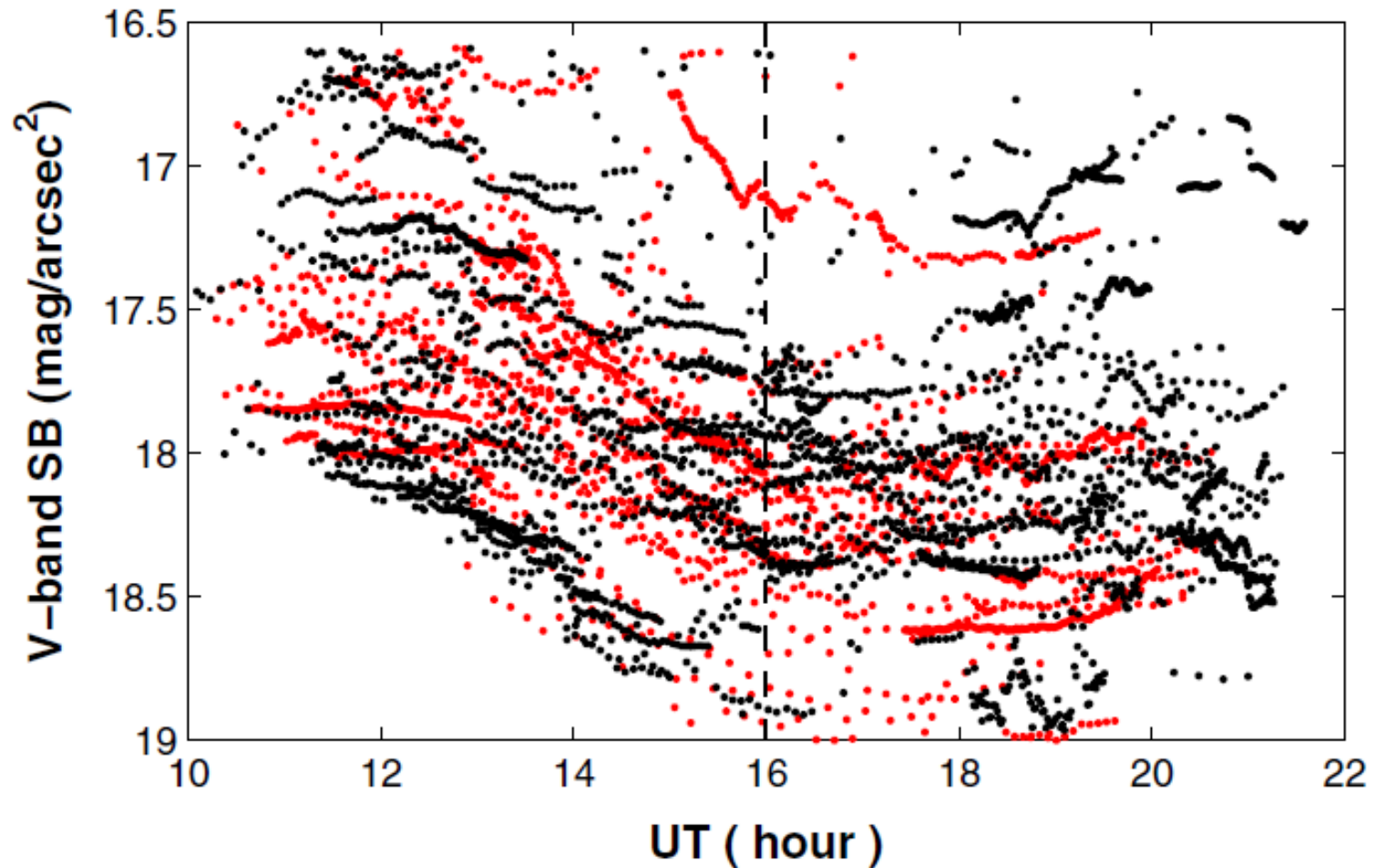
Monthly observatinal hours

Sky background



See Guo et al., PASP, 126, 496, 2014

Sky background



See Guo et al., PASP, 126, 496, 2014



Outline



- Motivation
- Brief introduction to Weihai observatory
- Blazar observations and variability research



Blazar observations



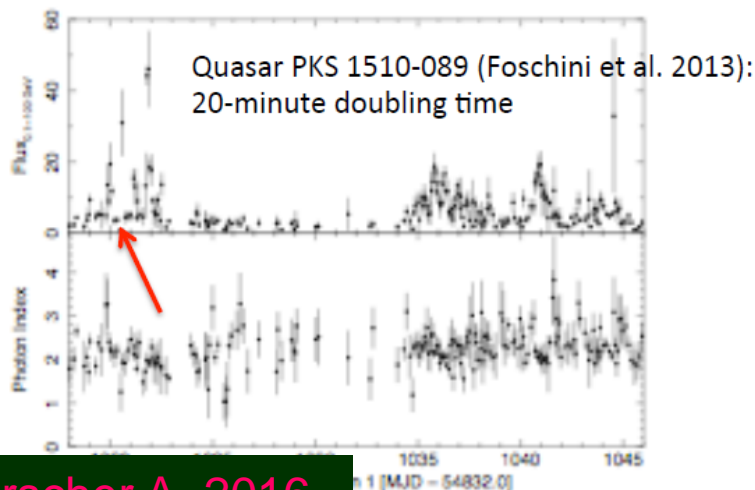
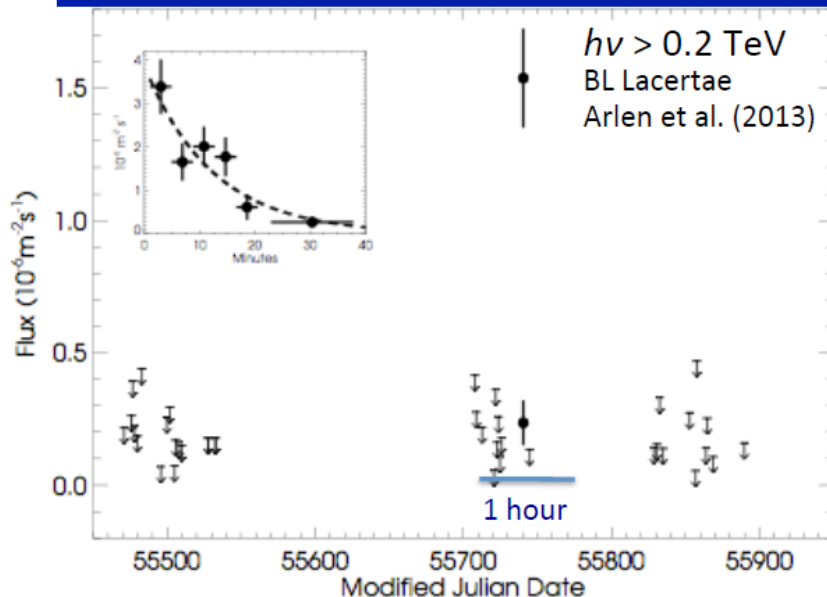
Objects	Data(Bands)	Nights
0109+224		
S5 0716+714	4584(V R I)	37
BL Lac	3865(V R I)	43
OT 546	1085(V R I)	23
PKS 1424+240	4066(V R I)	42
OI 090.4	794(V R I)	21
Mrk 421	2882(V R I)	41
3C 66A	3000(V R I)	44
3C 371	380(V R I)	6
ON 231	194(V R I)	3
0954+658		
1011+496		
1246+586		
OJ 287		



Microvariability study



Problem: Intra-day Variability on Parsec Scales



Changes in flux are observed to occur on time-scales t_{var} as short as minutes

How can this occur parsecs from the black hole?

Size of region needs to be smaller than ct_{var}
 $[\delta/(1+z)] \sim 2 \times 10^{14} t_{\text{var,hr}} \delta \text{ cm},$

where z is the redshift of the host galaxy and δ is the Doppler factor (blueshift) from relativistic motion of plasma

Superluminal motion implies $\delta \sim 20 - 50$

+ Jet is very narrow ($\sim 0.1/\Gamma_{\text{flow}}$; Jorstad et al. 2005, Clausen-Brown et al. 2013) so jet width 1 pc from black hole $\sim 10^{17} \text{ cm}$

+ Only some fraction of jet x-section is bright at any given time

→ Magnetic reconnection jet-in-jet model (Giannios 2013, MNRAS), or turbulence (Narayan & Piran 2012, MNRAS; Marscher 2012, Fermi and Jansky proc.)



Microvariability study



Duty cycle of microvariability for LBL:

BL Lac is 73%

0716+714 is 83.9%

OI 090.4 is 70%

Duty cycle of microvariability for HBL:

No significant IDV was found for OT 546 and Mrk 421

- Statistically the duty cycle of HBL is much lower than that of LBL. Why?
- Is it due to the stronger magnetic field of HBL to constrain the microvariability?

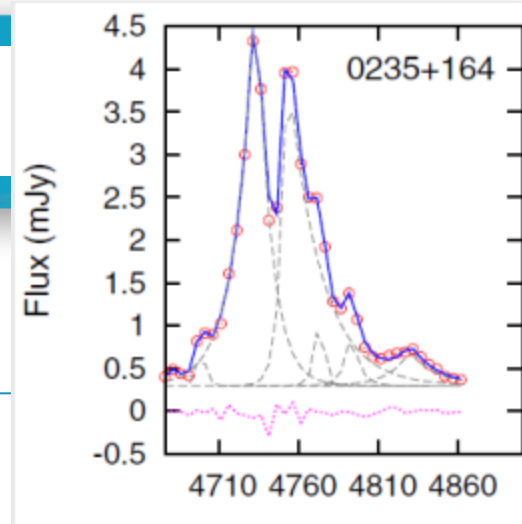
- Hu et al. 2006, MNRAS, 373, 209
- Hu et al., 2014, MNRAS, 443, 2940
- Hu et al., 2014, JAp&A, 35, 261
- Guo et al., 2014, JAp&A, 35, 283
- Chen et al., 2014, JAp&A, 35, 465

Statistical analysis for blazar flares

The light curves could be decomposed into individual flares using fitting methods.

Valtaoja (1999)

$$\Delta S(t) = \begin{cases} \Delta S_{\max} e^{(t-t_{\max})/\tau}, & t < t_{\max} \\ \Delta S_{\max} e^{(t_{\max}-t)/1.3\tau}, & t > t_{\max} \end{cases}$$



2012-AJ-749:191

Abdo (2010)

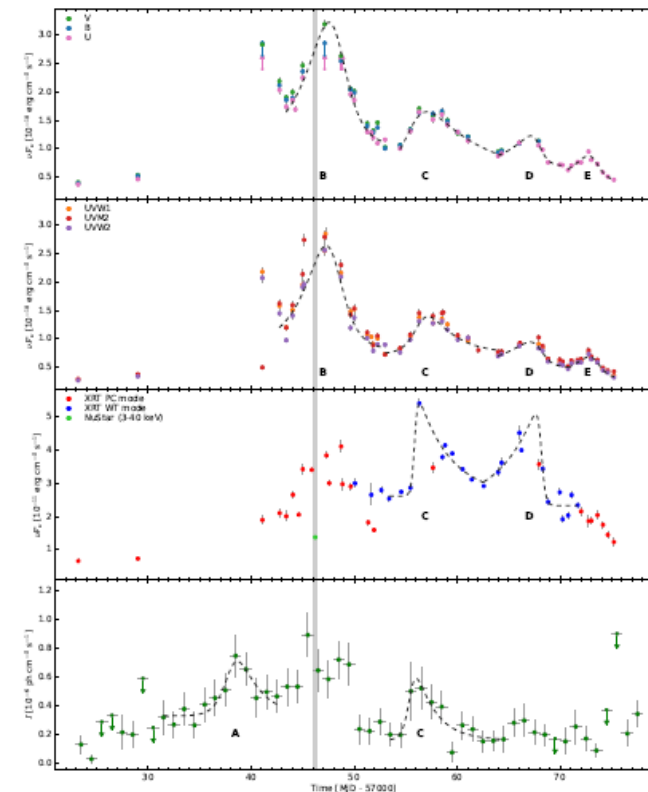
$$F(t) = F_c + F_0 \frac{1}{e^{(t_0-t)/T_r} + e^{(t-t_0)/T_d}}$$

Chatterjee (2012)

$$f(t) = f_0 + f_{\max} \times \exp[(t - t_0)/T_r], t < t_0$$

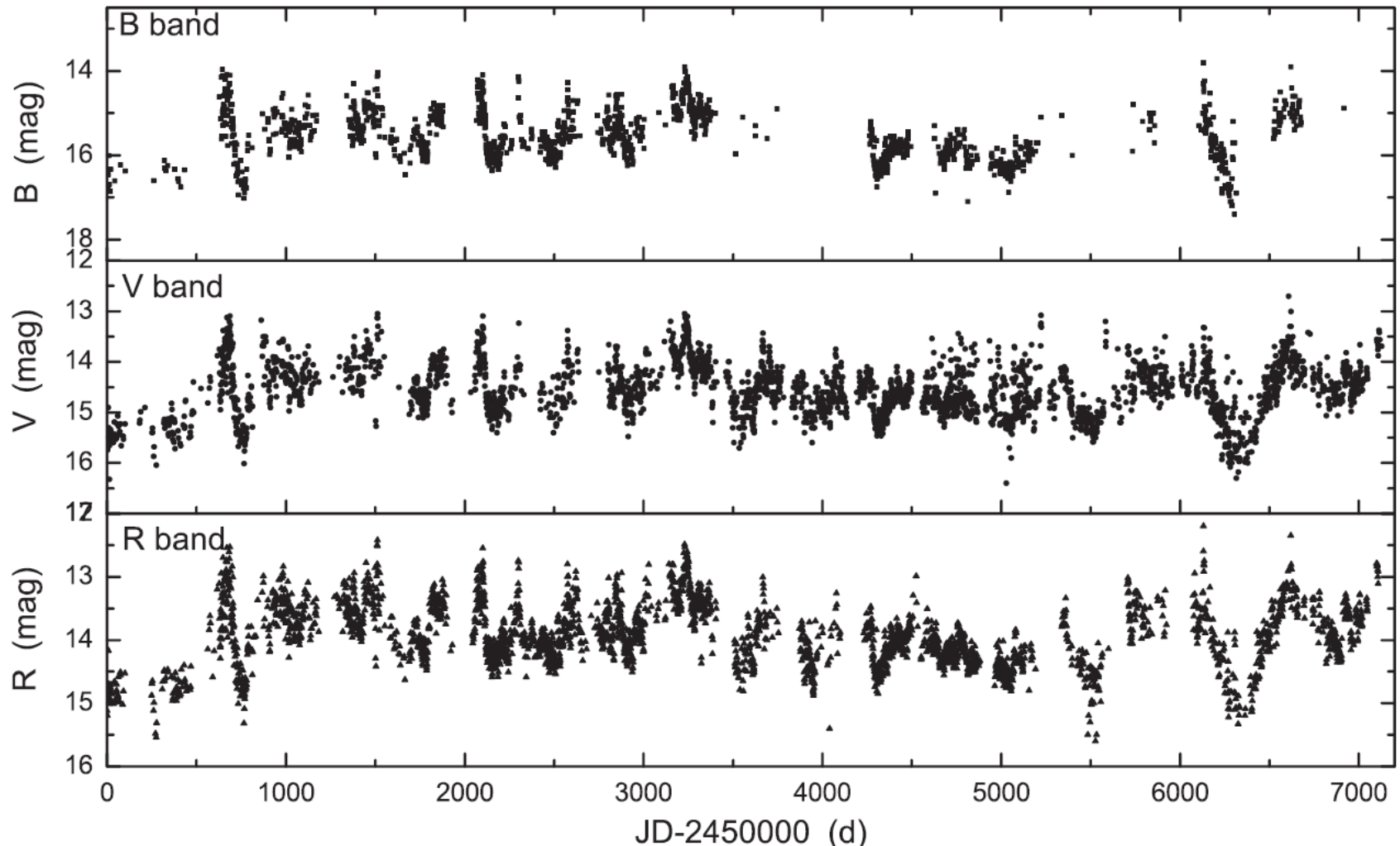
$$= f_0 + f_{\max} \times \exp[-(t - t_0)/T_d], t > t_0$$

Wierzcholska(2016)



Results for BL Lac

Optical light curves of BL Lacertae in B, V and R bands



See Guo, Hu et al. 2016, MNRAS, 460, 1790

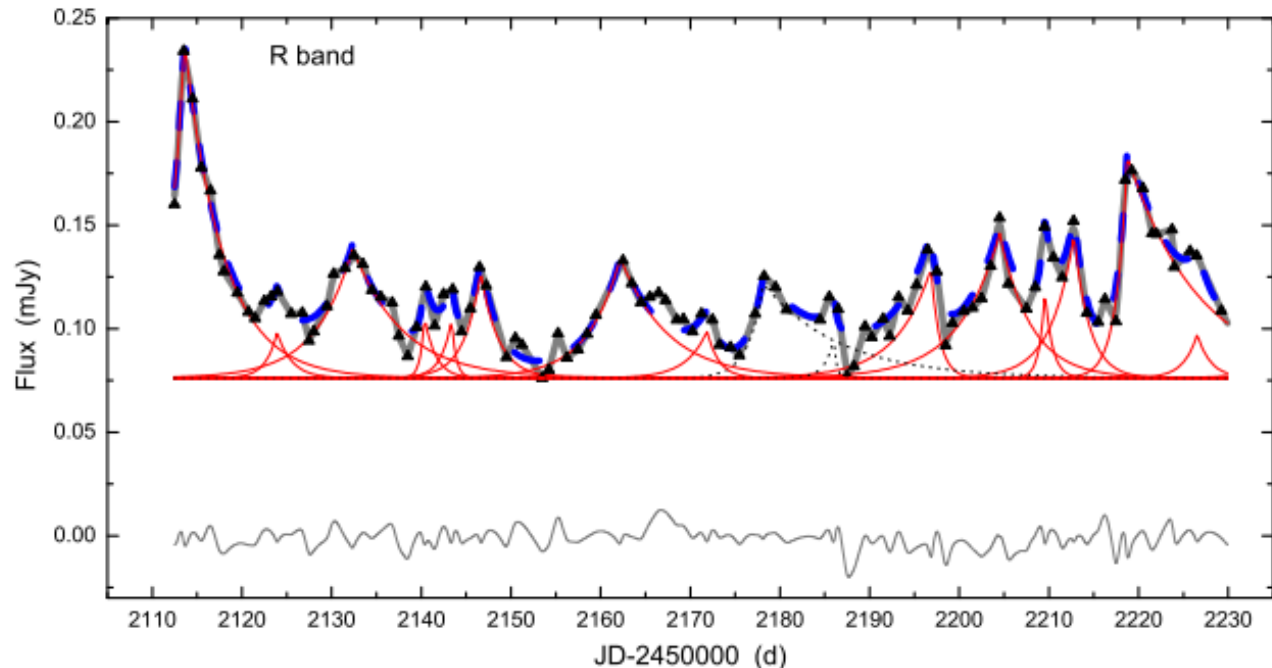
Flare fitting

- We adopted an exponential function introduced by Valtaoja et al. (1999) to decompose the flares.

$$f(t) = \begin{cases} f_0 + f_{max} \exp[(t - t_0)/T_r], & \text{for } t < t_0 \text{ and} \\ f_0 + f_{max} \exp[-(t - t_0)/T_d], & \text{for } t > t_0 \end{cases}$$

- Before the fitting of flares, all segments were interpolated linearly by a time interval τ_{in} , then smoothed by a Gaussian function with particular FWHM

In order to optimize the fitting of flares and obtain the best result, different segment was applied to different τ_{in} and FWHM.



Properties of Flares

- Flare duration time

$$T \simeq 2(T_r + T_d)$$

- Skewness parameter

$$\xi = \frac{T_d - T_r}{T_d + T_r}$$

- Amplitude of flare

$$f_{max}$$

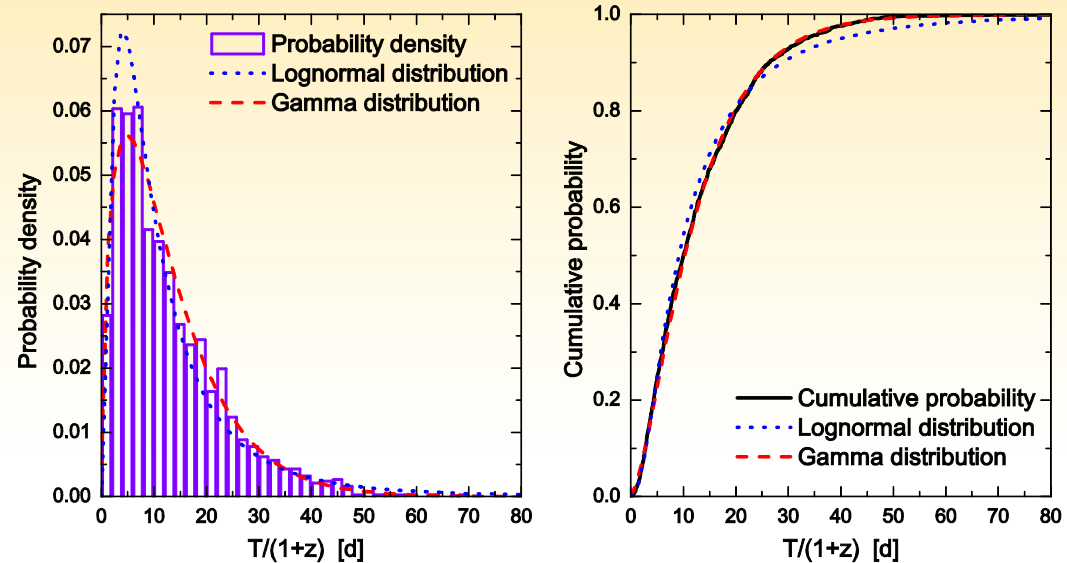
- Energy output

$$Area = \int_{-\infty}^{+\infty} f(t) - f_0 dt = f_{max}(t_r + t_d)$$

Flare duration



- The probability density and cumulative probability of $T/(1+z)$ are shown. Gamma distribution seemed to be appropriate to explain this distribution according to K-S test.
- lognormal distribution



$$f(x|\mu, \sigma) = \frac{1}{\sqrt{2\pi}\sigma x} e^{-\frac{(\ln x - \mu)^2}{2\sigma^2}}$$

- gamma distribution

$$f(x|a, b) = \frac{1}{b^a \Gamma(a)} x^{a-1} e^{-\frac{x}{b}}$$

		Lognormal distribution			Gamma distribution		
band		μ	σ	h	a	b	h
$T/(1+z)$	all	2.212 ± 0.021	0.897 ± 0.015	1	1.610 ± 0.048	7.978 ± 0.280	0
f_{max}	V	-2.774 ± 0.024	0.710 ± 0.017	0	2.178 ± 0.099	0.037 ± 0.002	1
	R	-2.597 ± 0.029	0.773 ± 0.021	0	1.797 ± 0.089	0.056 ± 0.003	1
Area	V	-1.214 ± 0.045	1.319 ± 0.032	0	0.764 ± 0.032	0.849 ± 0.049	1
	R	-0.967 ± 0.048	1.254 ± 0.034	0	0.840 ± 0.039	0.913 ± 0.057	1

VARIABILITY ANALYSIS RESULTS

—Flare asymmetry

- Distributions of ξ are presented in the plot. The red line in each panel presents the result of Gaussian fitting. Mean and standard deviation of the Gaussian function (μ and σ , respectively) are listed in table 1.
- Despite different τ_{in} and FWHM shown in table 1, μ were slightly less than zero within the statistical uncertainties, reflecting that **there might be a trend toward gradual rises and rapid decays**. Or we could safely say that no or at most very weak negative asymmetry were found in the variations of BL Lacertae.

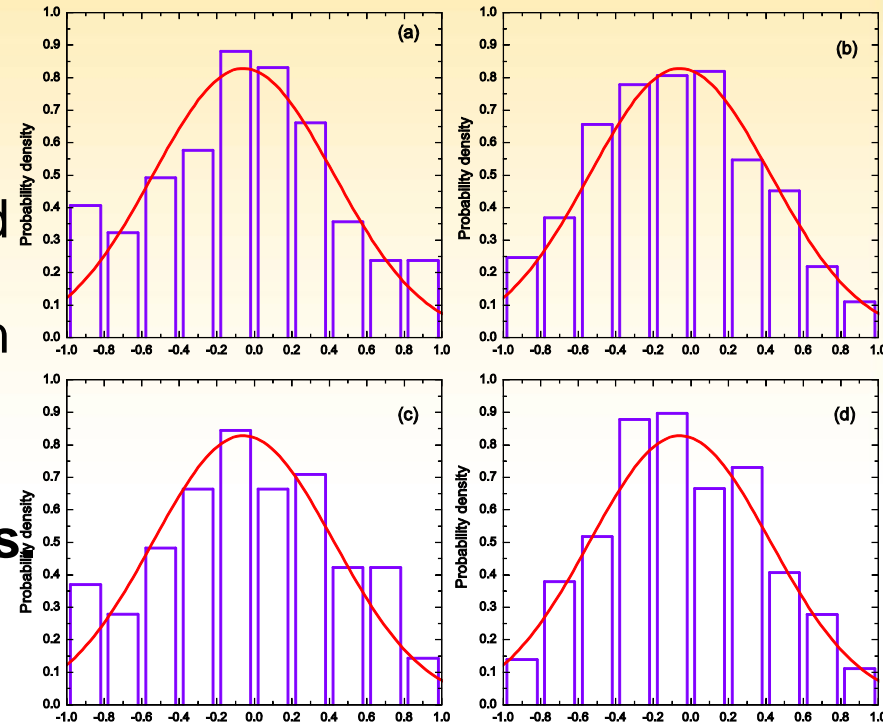
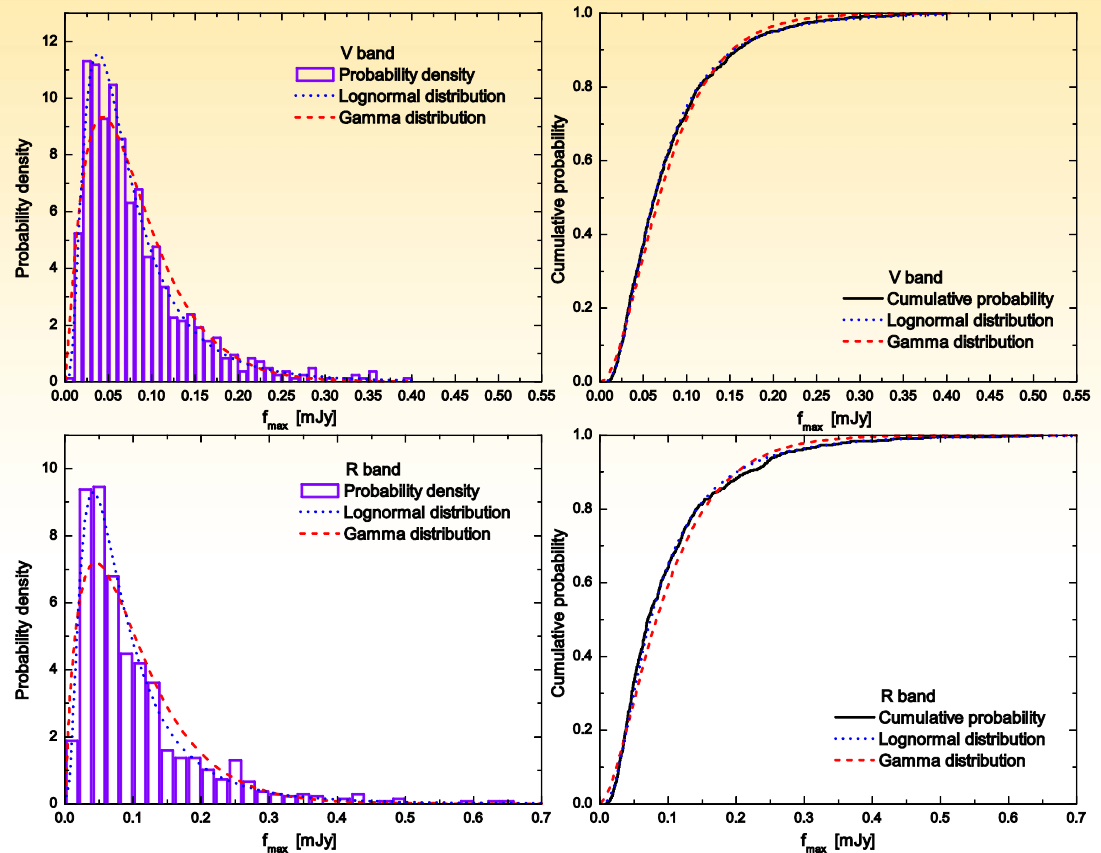


Table 1. Statistics of flares.

type	linear interpolation	gauss smoothing	number of flares				Gaussian Fitting		$-0.3 < \xi < 0.3$	$0.3 < \xi < 0.7$	$0.7 < \xi < 1$
	τ_{in}	FWHM	B band	V band	R band	sum	μ	σ			
a	0.5 ~ 1	1	20	195	80	295	-0.058 ± 0.028	0.482 ± 0.020	47.5%	33.2%	19.3%
b	0.5 ~ 1	5	37	214	115	366	-0.080 ± 0.023	0.437 ± 0.016	47.3%	40.7%	12.0%
c	0.1 ~ 0.5	1	147	273	243	663	-0.030 ± 0.019	0.479 ± 0.013	44.6%	38.5%	16.9%
d	0.1 ~ 0.5	5	120	166	255	541	-0.047 ± 0.018	0.421 ± 0.013	50.3%	39.2%	10.5%

Peak flux of flares

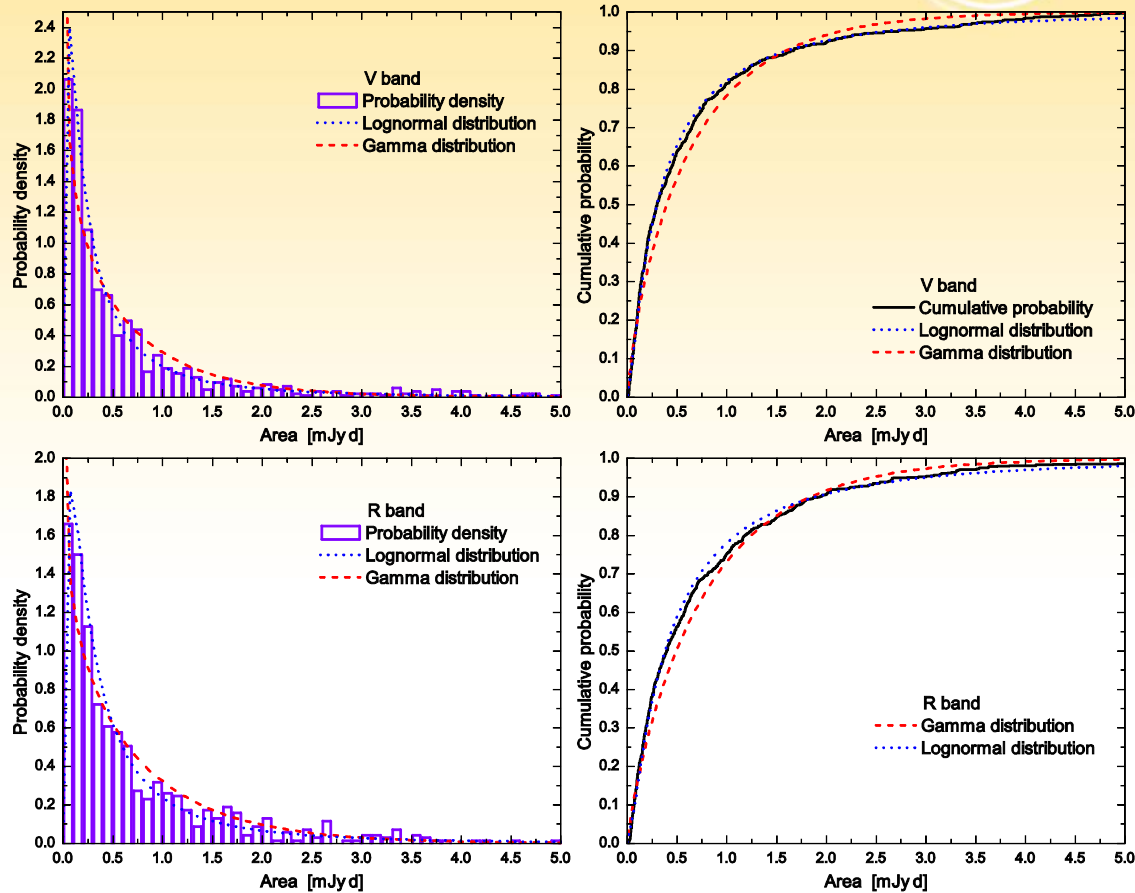
- The probability density and cumulative probability of f_{\max} of the flares in V bands and R bands are depicted in the plots. Lognormal distribution seemed to be more precise to explain the distribution of f_{\max} .



	band	Lognormal distribution			Gamma distribution		
		μ	σ	h	a	b	h
$T/(1+z)$	all	2.212 ± 0.021	0.897 ± 0.015	1	1.610 ± 0.048	7.978 ± 0.280	0
f_{\max}	V	-2.774 ± 0.024	0.710 ± 0.017	0	2.178 ± 0.099	0.037 ± 0.002	1
	R	-2.597 ± 0.029	0.773 ± 0.021	0	1.797 ± 0.089	0.056 ± 0.003	1
Area	V	-1.214 ± 0.045	1.319 ± 0.032	0	0.764 ± 0.032	0.849 ± 0.049	1
	R	-0.967 ± 0.048	1.254 ± 0.034	0	0.840 ± 0.039	0.913 ± 0.057	1

Energy output of fares

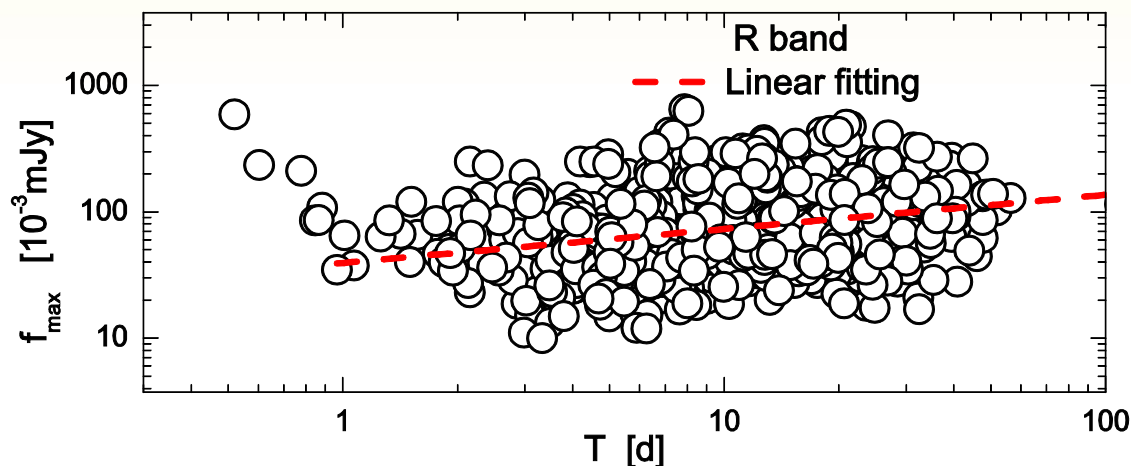
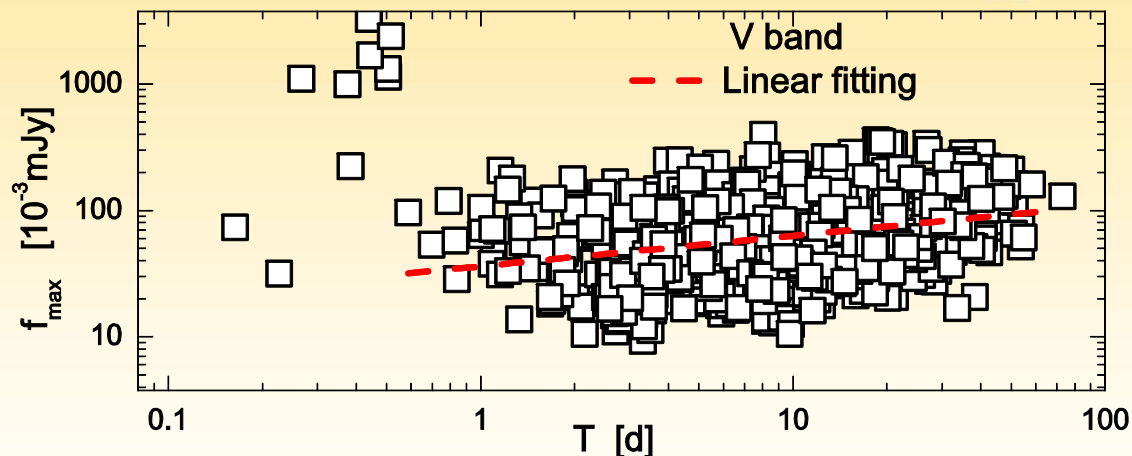
- The probability density and cumulative probability of Area in V bands and R bands are depicted. Lognormal distribution seemed to be more precise to explain the distribution of f_{max} .



		Lognormal distribution			Gamma distribution		
band		μ	σ	h	a	b	h
$T/(1+z)$	all	2.212 ± 0.021	0.897 ± 0.015	1	1.610 ± 0.048	7.978 ± 0.280	0
	V	-2.774 ± 0.024	0.710 ± 0.017	0	2.178 ± 0.099	0.037 ± 0.002	1
	R	-2.597 ± 0.029	0.773 ± 0.021	0	1.797 ± 0.089	0.056 ± 0.003	1
f_{max}	V	-1.214 ± 0.045	1.319 ± 0.032	0	0.764 ± 0.032	0.849 ± 0.049	1
	R	-0.967 ± 0.048	1.254 ± 0.034	0	0.840 ± 0.039	0.913 ± 0.057	1
Area	V						
	R						

Correlation between T and fmax

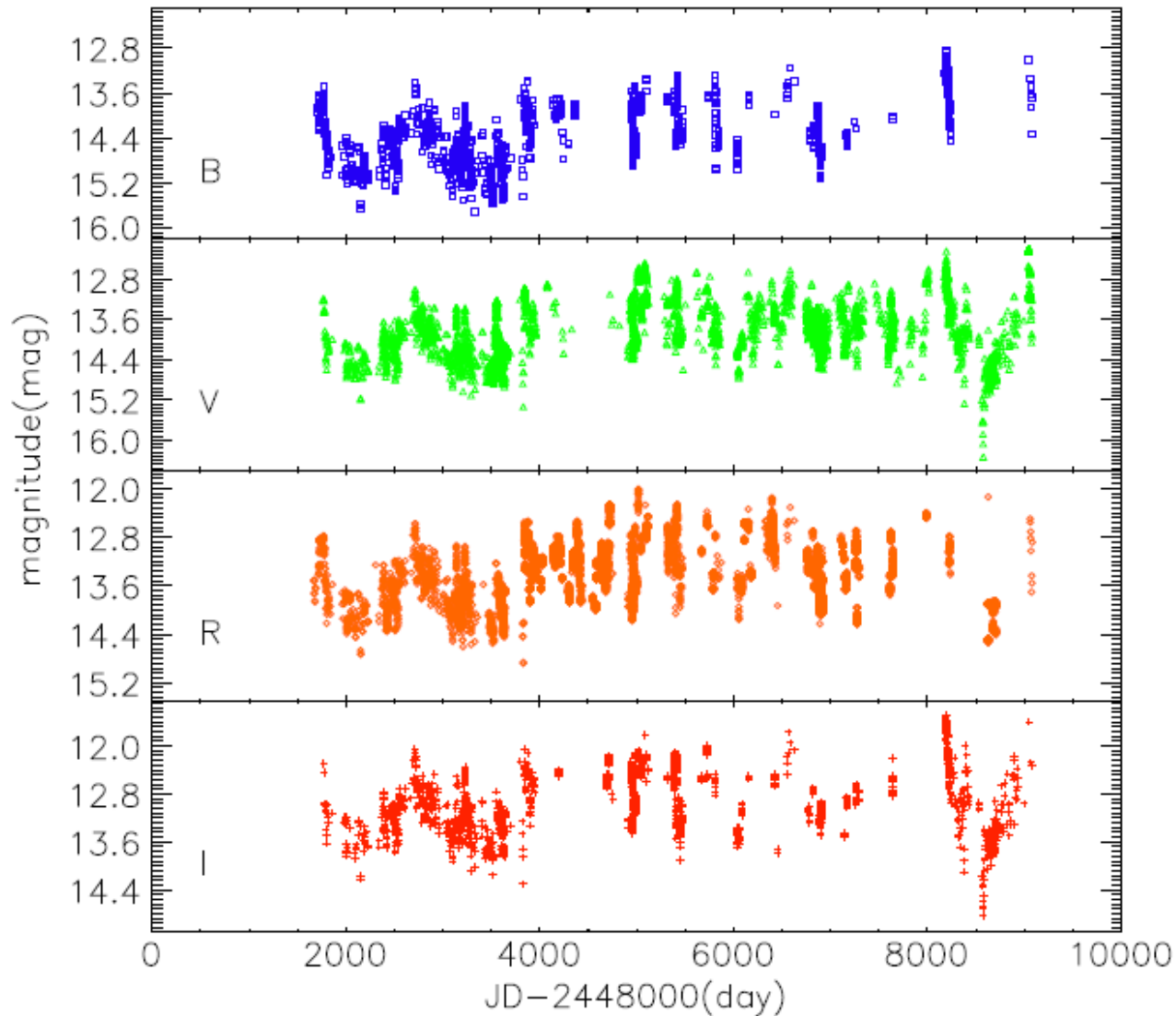
- Despite the divergency, there is a clear correlation that fmax becomes larger with a larger T.



$$\log(f_{\max}^V) \propto (0.241 \pm 0.026)\log(T)$$

$$\log(f_{\max}^R) \propto (0.269 \pm 0.035)\log(T)$$

Results for 0716



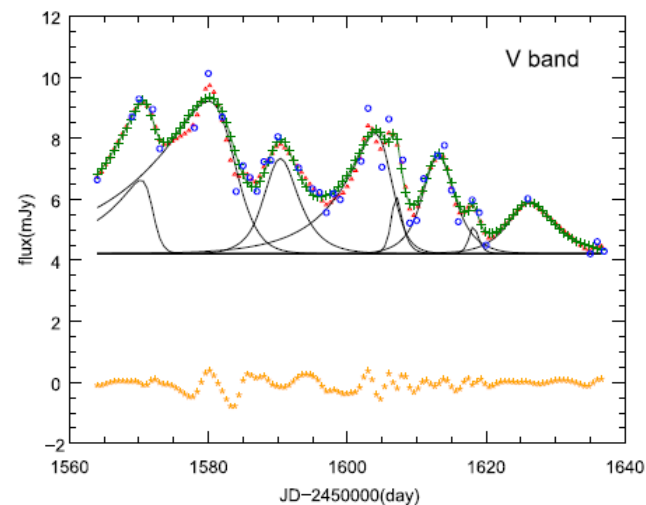
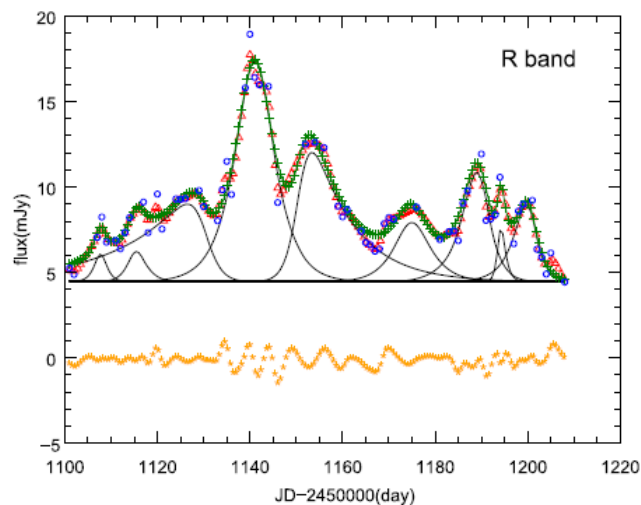
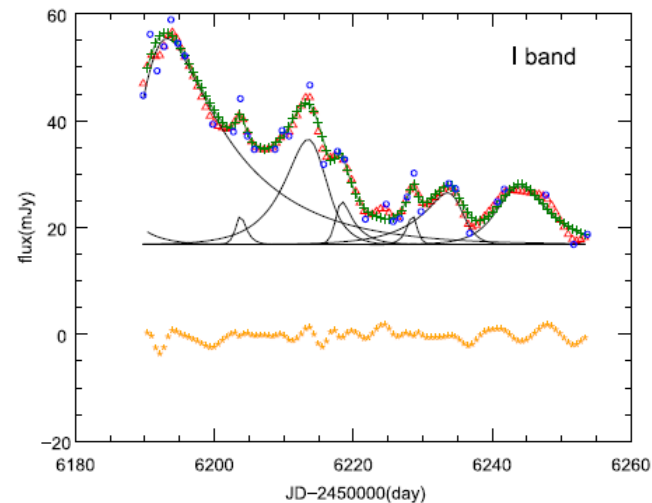
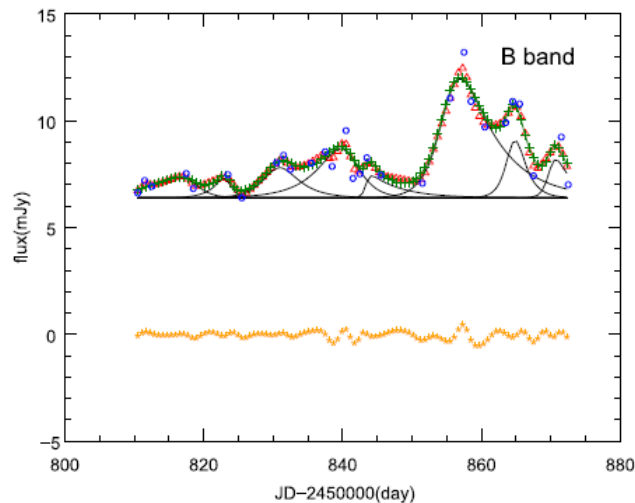
See Li, Hu et al. 2017, PASP, 129, 4101

Temporal Structure of S5 0716+714

➤ Flares of Short-term Light Curves

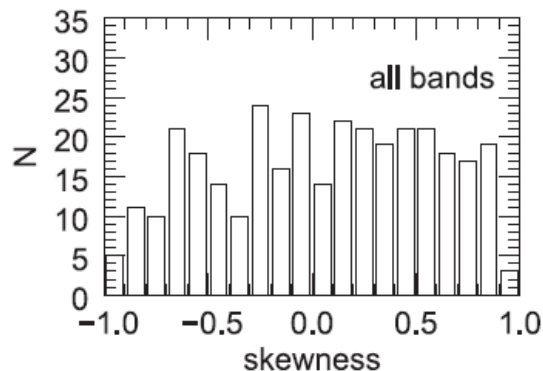
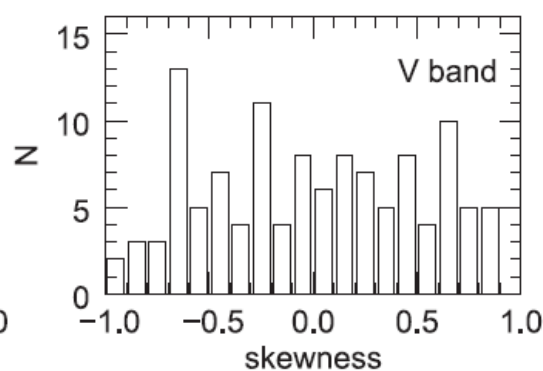
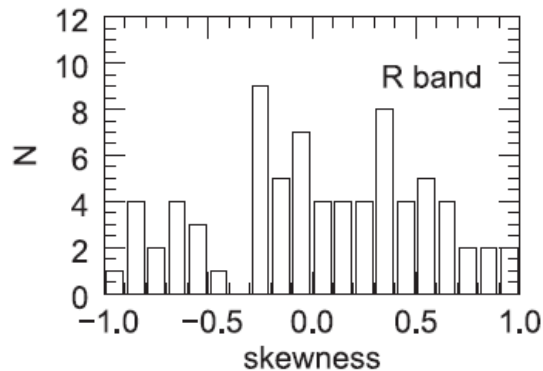
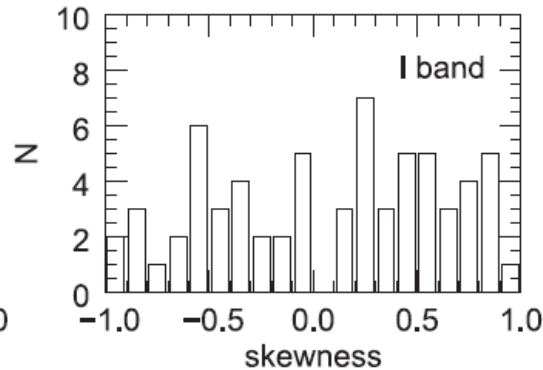
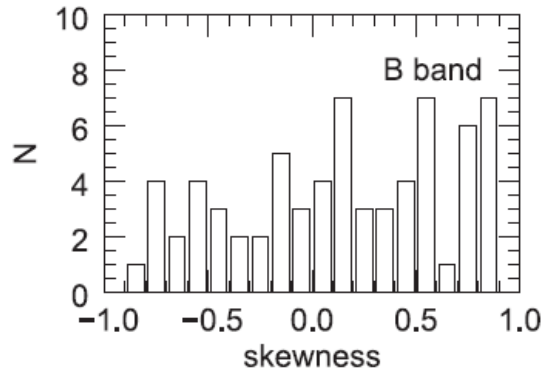
$$f(t) = f_0 + f_{max} \times \exp[(t - t_0)/T_r], t < t_0$$

$$= f_0 + f_{max} \times \exp[-(t - t_0)/T_d], t > t_0$$





Skewness-STV



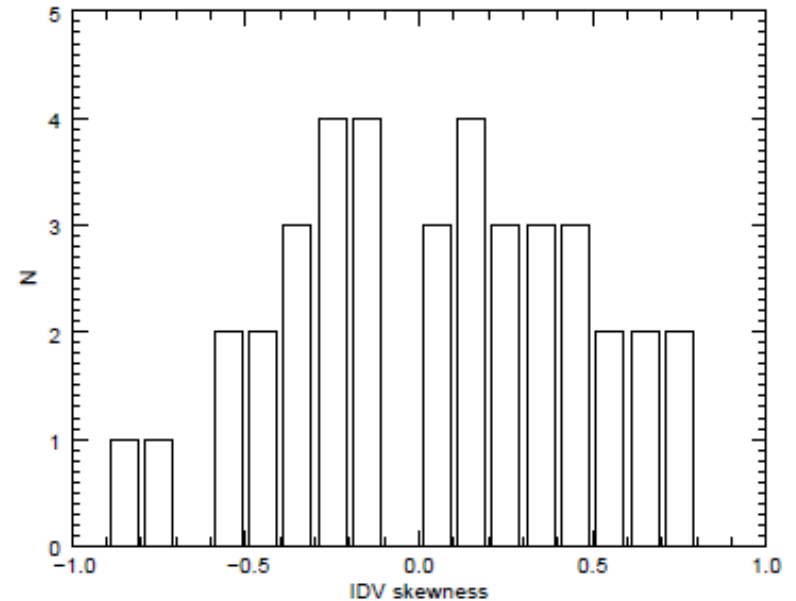
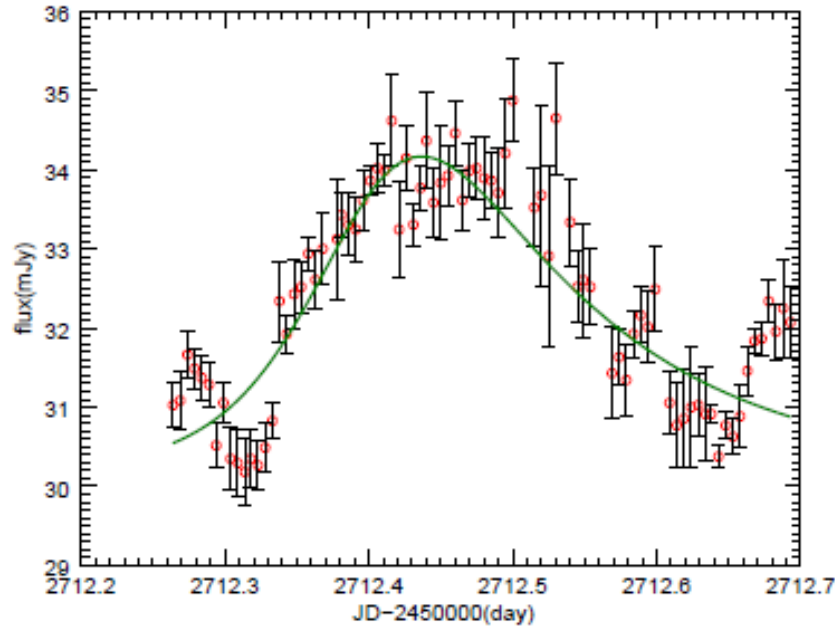
The results show that the flares are predominantly asymmetric in four bands. there exists a very weak tendency of positive asymmetry with rapid rises and gradual decays.

Table 1
Number of Flares and Percentage of $|\xi|$ in Each Band

Band	Flare Num.	<0.3	0.3 ~ 0.7	0.7 ~ 1.0
<i>B</i>	68	35.3%	38.2%	26.5%
<i>V</i>	66	28.8%	47.0%	24.2%
<i>R</i>	75	44.0%	38.7%	17.3%
<i>I</i>	118	37.3%	47.5%	15.2%
All	327	36.7%	43.4%	19.9%

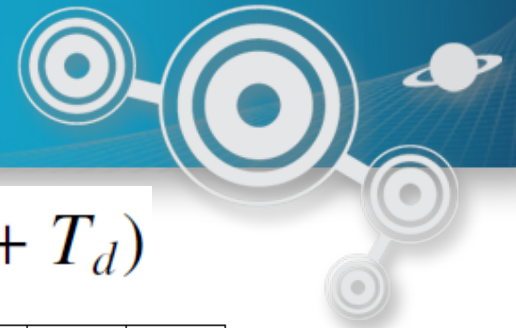


Skewness-IDV



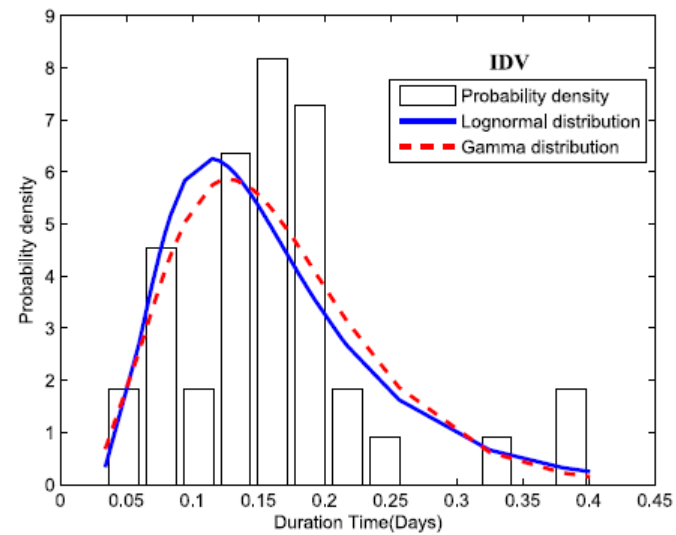
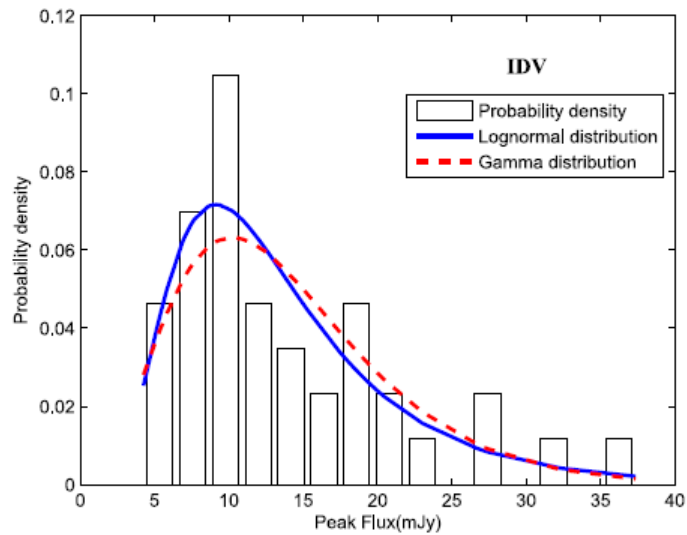
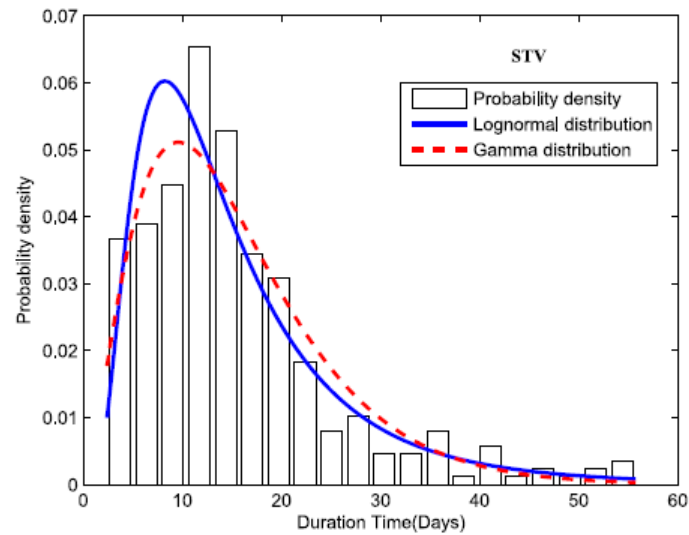
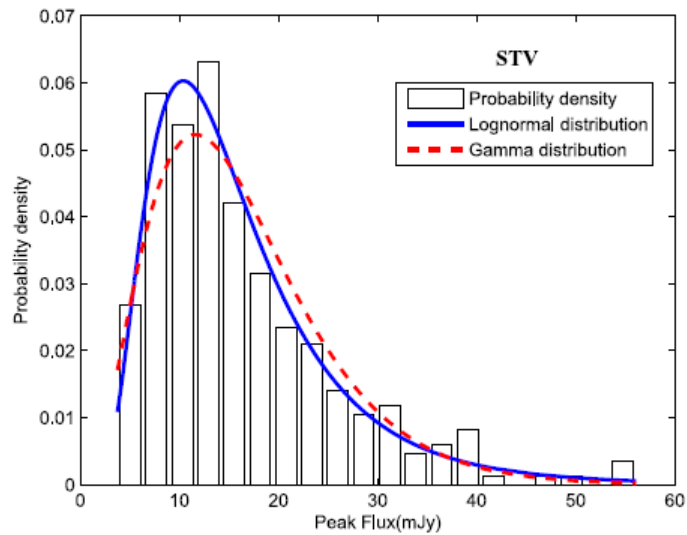
Band	skewness percentage $ \xi $		
	< 0.3	0.3 ~ 0.7	0.7 ~ 1.0
All	46.2%	43.6%	10.2%

Both STV and IDV flares were predominantly asymmetric. But the percentage of symmetric flares for IDV is higher than STV.



$$f_p = f_0 + f_{max}$$

$$T \simeq 2(T_r + T_d)$$



the Fig.1 of [Biteau et al. \(2012\)](#). For a large number of minijets, typically $N \geq 10^3$, the distribution of the logarithm of the flux can be described with a peak, followed by a power-law tail, which could be interpreted very well as a log-normal distribution. The statistics of S5 0716+714 in peak

- The Log-normal distribution of the flux suggests that the variability seems from multiplicative processes.
 - Maybe a minijets-in-a-jet statistical model
- ([Biteau et al. 2012](#))
- The Gamma distribution could demonstrate that the emission region in the jet may be distributed in a Poisson way.

([Touati et al. 2009](#))



Discussions



A power law function, continuously injected for $t_{inj} \sim R/c$.

$\tau_{cool} \ll R/c$ symmetric light curves

$\tau_{cool} \gg R/c$ asymmetric light curves

For symmetric light curves:

$t < R/c$ flux increase

$t > R/c$ flux decrease

MNRAS,1999,306,551



Discussions



$$\tau_{syn} = \frac{3m_e c}{4\sigma_T U_B \gamma}$$

$$U_B = \frac{B^2}{8\pi}$$

$$\tau_{cool} = \frac{7.7 \times 10^8}{\gamma B^2} s$$

Chen et al. ,MNRAS, 2011,416, 2368

For blazar S5 0716+714, [Ghisellini et al. \(1997\)](#) derived the magnetic field and gamma in homogeneous synchrotron self Compton model with $B = 0.48$ (or $B = 0.84$) Gauss, and $\gamma_{min} = 3 \times 10^3$, $\gamma_{max} = 10^5$. Therefore, with the Equation 6, we can calculate the cooling time range is $3.3 \times 10^4 \sim 1.1 \times 10^6 s$ ($B = 0.48$) or $1.1 \times 10^4 \sim 3.6 \times 10^5 s$ ($B = 0.84$).



Discussions



$$\tau_{cool} = 6.2 \times 10^4 \sim 3.1 \times 10^6 s$$

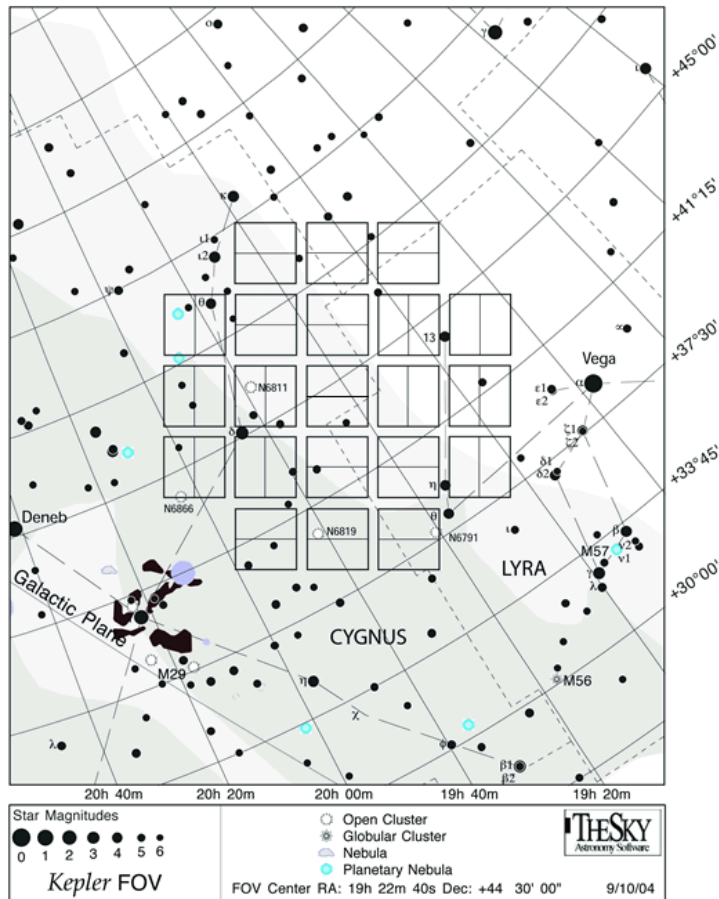
Table 2
The Estimated Parameters of the Flares

Parameters	STV	IDV
Duration Time T (s)	$2.1 \times 10^5 \sim 4.8 \times 10^6$	$5.9 \times 10^3 \sim 6.9 \times 10^4$
Median of Duration Time T_m (s)	1.1×10^6	2.6×10^4
Light Travel Time T_j (s)	$8.0 \times 10^5 \sim 1.1 \times 10^8$	$2.2 \times 10^4 \sim 1.6 \times 10^6$
Peak Flux F_p (mJy)	$3.8 \sim 56.1$	$4.3 \sim 37$
Median of Peak Flux f_m (mJy)	13.7	10.9
Emission Size R (cm)	$2.4 \times 10^{16} \sim 3.3 \times 10^{18}$	$6.6 \times 10^{14} \sim 4.8 \times 10^{16}$

The symmetric nature of the observed flares indicates that the skewness profiles can not just explained by a disturbance through the emission region or crossing time effect, light travel time effect. Meanwhile it may also be constrained by geometric effect and other effects.



Kepler blazar sources



Information:

- **Very good time coverage**
- **0.95-meter aperture**

BL Lac :

KIC 6690887--W2R 1926+42

KIC 7175757--5BZBJ1848+4245



Multiband analysis



P2-03 A Multiwavelength Study of Mrk 421

Xu Chen (Shandong U.)

P2-04 Spectral and correlation analysis of multiple wavelength for blazar PMN J2345-1555

Yunguo Jiang (Shandong U.)



A&A 558, A92 (2013)
DOI: 10.1051/0004-6361/201220236
© ESO 2013

The 72-h WEBT micro of blazar S5 071

G. Bhatta¹, J. R. Webb¹, H. Hollingsworth¹, S. Dhalla¹,
O. J. A. Bravo Calle⁴, P. Calciolase⁶, D. Capezzali⁷, D. C.
Y. Efimov¹³, A. C. Gupta¹⁴, S.-M. Hu¹⁵, O. Kurtanidze¹⁶,
E. Lindfors²⁰, B. Murphy²¹, K. Nilsson²⁰, J. M. Ohlert²²,
R. Reinthal²⁰, D. Rodriguez²⁶, J. A. Ros²⁷, P. Roustazadeh²⁸,
A. Strigachev², L. Takalo²⁰, S. Vennes²⁹, M. Vi

(Affiliations can be found

Received 15 August 2012.

ABST

Context. The international Whole Earth Blazar Telescope (WEBT) consists of observations of S5 0716+714 from February 22, 2009 to February 25, 2010, its high declination, and its very large duty cycle for micro-variations.

Aims. We report here on the long continuous optical micro-variability light curve during which the Blazar showed almost constant variability over a 0.5 m. Observations from participating observatories were corrected for instrumental effects.

Methods. Thirty-six observatories in sixteen countries participated in this compilation into a continuous light curve. The light curve was analyzed using analysis techniques. Those results led us to model the light curve by attributing the observed micro-variations in this extended light curve to cells in a turbulent jet which are energized by a passing shock. We have interpreted the observed micro-variations in this extended light curve fit to the 72-hour light curve with the synchrotron pulse model.

Key words. quasars: individual: S5 0716+714 – BL Lacertae objects: individual: S5 0716+714

Monthly Notices

of the
ROYAL ASTRONOMICAL SOCIETY

MNRAS **469**, 2457–2463 (2017)
Advance Access publication 2017 May 4

doi:10.1093/mnras/stx1062

Radio and optical intra-day variability observations of five blazars

X. Liu,^{1,2★} P. P. Yang,^{1,3} J. Liu,^{1,2★} B. R. Liu,⁴ S. M. Hu,⁵ O. M. Kurtanidze,^{6,7,8}
S. Zola,^{9,10} A. Kraus,¹¹ T. P. Krichbaum,¹¹ R. Z. Su,^{1,3} K. Gazeas,¹² K. Sadakane,¹³
K. Nilson,¹⁴ D. E. Reichart,¹⁵ M. Kidger,¹⁶ K. Matsumoto,¹³ S. Okano,¹⁷ M. Siwak,¹⁰
J. R. Webb,¹⁸ T. Pursimo,¹⁹ F. Garcia,²⁰ R. Naves Nogueira,²¹ A. Erdem,^{22,23}
F. Alicavus,^{22,23} T. Balonek²⁴ and S. G. Jorstad²⁵

Affiliations are listed at the end of the paper

Accepted 2017 April 28. Received 2017 April 18; in original form 2017 March 14

MULTIFREQUENCY PHOTO-POLARIMETRIC WEBT OBSERVATION CAMPAIGN ON THE BLAZAR S5 0716+714: SOURCE MICROVARIABILITY AND SEARCH FOR CHARACTERISTIC TIMESCALES*

G. BHATTA¹, L. STAWARZ¹, M. OSTROWSKI¹, A. MARKOWITZ², H. AKITAYA³, A. A. ARKHAROV⁴, R. BACHEV⁵, E. BENÍTEZ⁶,
G. A. BORMAN⁷, D. CAROSATI^{8,9}, A. D. CASON¹⁰, R. CHANISHVILI¹¹, G. DAMIJANOVIC¹², S. DHALLA¹³, A. FRASCA¹⁴, D. HIRIART¹⁵,
S.-M. HU¹⁶, R. ITOH¹⁷, D. JABLEKA¹, S. JORSTAD^{18,19}, M. D. JOVANOVIĆ²⁰, K. S. KAWABATA²¹, S. A. KLIMANOV²²,
O. KURTANIDZE^{11,20,21}, V. M. LARIONOV^{4,19}, D. LAURENCE¹³, G. LETO¹⁴, A. P. MARSCHER¹⁸, J. W. MOODY²², Y. MORITANI²³,
J. M. OHLERT²⁴, A. DI PAOLA²⁵, C. M. RAITERI²⁶, N. RIZZI²⁷, A. C. SADUN²⁸, M. SASADA¹⁸, S. SERGEEV⁷, A. STRIGACHEV⁵,
K. TAKAKI¹⁷, I. S. TROITSKY¹⁹, T. U¹⁷, M. VILLATA²⁶, O. VINCE¹², J. R. WEBB¹³, M. YOSHIDA³, AND S. ZOLA^{1,29}

¹Astronomical Observatory of Jagiellonian University, ul. Orla 171, 30-244 Krakow, Poland; gopalbhatta716@gmail.com
²Center for Astrophysics and Space Sciences, University of California, San Diego, 9500 Gilman Dr., La Jolla, CA 92093-0424, USA

³Hiroshima Astrophysical Science Center, Hiroshima University, Higashi-Hiroshima, Hiroshima 739-8526, Japan

⁴Main (Pulkovo) Astronomical Observatory of RAS, Pulkovskoye shosse, 60, 196140 St. Petersburg, Russia

⁵Institute of Astronomy, Bulgarian Academy of Sciences, 72, Tzarigradsko Shosse Blvd., 1784 Sofia, Bulgaria

⁶Instituto de Astronomía, Universidad Nacional Autónoma de México, México DF, México

⁷Crimean Astrophysical Observatory, P/O Nauchny, Crimea, 298409, Russia

⁸EPT Observatories, Tjarafé, La Palma, Spain

⁹INAF, TNG Fundación Galileo Galilei, La Palma, Spain

¹⁰Private address, 105 Glen Pine Trail, Dawsonville, GA 30534, USA

¹¹Abastumani Observatory, Mt. Kanobili, 0301 Abastumani, Georgia

¹²Astronomical Observatory, Volgina 7, 11060 Belgrade, Serbia

¹³Florida International University, Miami, FL 33199, USA

¹⁴INAF—Osservatorio Astrofisico di Catania, Italy

¹⁵Instituto de Astronomía, Universidad Nacional Autónoma de México, Ensenada, México

¹⁶Shandong Provincial Key Laboratory of Optical Astronomy and Solar-Terrestrial Environment, Institute of Space Sciences, Shandong University at Weihai, 264209 Weihai, China

¹⁷Department of Physical Science, Hiroshima University, Higashi-Hiroshima, Hiroshima 739-8526, Japan

¹⁸Institute for Astrophysical Research, Boston University, 725 Commonwealth Ave., Boston, MA 02215, USA

¹⁹Astronomical Institute, St. Petersburg State University, Universitetskij Pr. 28, Petrodvorets, 198504 St. Petersburg, Russia

²⁰Engelhardt Astronomical Observatory, Kazan Federal University, Tatarstan, Russia

²¹Landessternwarte Heidelberg-Königstuhl, Germany

²²Physics and Astronomy Department, Brigham Young University, N283 ESC, Provo, UT, 84602, USA

²³Kavli Institute for the Physics and Mathematics of the universe (Kavli PMU), The University of Tokyo, 5-1-5 Kashiwa-no-Ha, Kashiwa City Chiba, 277-8583, Japan

²⁴Astronomie Stiftung Tebur, Fichtenstrasse 7, D-65468 Trebur, Germany

²⁵INAF—Osservatorio Astronomico di Roma, via Frascati 33, I-00040 Monte Porzio, Italy

²⁶INAF—Osservatorio Astrofisico di Torino, Italy

²⁷Sirio Astronomical Observatory Castellana Grotte, Italy

²⁸Department of Physics, Univ. of Colorado Denver, CO, USA

²⁹Mt. Suhora Observatory, Pedagogical University, ul. Podchorążych 2, 30-084 Krakow, Poland

Received 2016 May 10; revised 2016 August 2; accepted 2016 August 10; published 2016 October 28

Welcome to visit Weihai observatory

A photograph of the Weihai Observatory building, featuring a prominent silver dome and a white rectangular structure, situated on a hill covered in green trees. A paved road leads up the hill towards the building. The sky is clear and blue.

Contact with Shao Ming Hu
Email: hushm@sdu.edu.cn

Thank you for your attention!